The Human Erythrocyte Anion Transport Protein, Band 3

Characterization of Exofacial Alkaline Titratable Groups Involved in Anion Binding/Translocation

POUL J. BJERRUM

From the Department of Clinical Chemistry, Herlev Hospital, University of Copenhagen, Copenhagen, Denmark

ABSTRACT Chloride self-exchange across the human erythrocyte membrane at alkaline extracellular pH (pH_o) and constant neutral intracellular pH (pH_i) can be described by an exofacial deprotonatable reciprocating anion binding site model. The conversion of the transport system from the neutral to the alkaline state is related to deprotonation of a positively charged ionic strength– and substrate-sensitive group. In the absence of substrate ions ($[Cl_o] = 0$) the group has a pK of ~9.4 at constant high ionic strength (equivalent to ~150 mM KCl) and a pK of ~8.7 at approximately zero ionic strength. The alkaline ping-pong system (examined at constant high ionic strength) demonstrates outward recruitment of the binding sites with an asymmetry factor of ~0.2, as compared with the inward recruitment of the transport system at neutral pH_o with an asymmetry factor of ~10. The intrinsic half-saturation constant for chloride binding, with $[Cl_i] = [Cl_o]$, increases from ~30 mM at neutral to ~110 mM at alkaline pH_o. The maximal transport rate was a factor of ~1.7 higher at alkaline pH_o. This increase explains the stimulation of anion transport, the "modifier hump," observed at alkaline pH_o. The translocation of anions at alkaline pH_o was inhibited by deprotonation of another substrate-sensitive group with an intrinsic pK of ~11.3. This group together with the group with a pK of ~9.4 appear to form the essential part of the exofacial anion binding site. The effect of extracellular iodide inhibition on chloride transport as a function of pH_o could, moreover, be simulated if three extracellular iodide binding constants were included in the model: namely, a competitive intrinsic iodide binding constant of ~1 mM in the neutral state, a self-inhibitor binding constant of ~120 mM in the neutral state, and a competitive intrinsic binding constant of ~38 mM in the alkaline state.

INTRODUCTION

The exchange of monovalent and divalent anions through the red cell membrane is mediated by an integral trans-membrane protein (Cabantchik and Rothstein, 1974)

Address reprint requests to Dr. Poul J. Bjerrum, Department of Clinical Chemistry, Herlev Hospital, University of Copenhagen, Herlev Ringvej 75, DK-2730 Herlev, Denmark.

J. GEN. PHYSIOL. © The Rockefeller University Press · 0022-1295/92/08/0301/39 $2.00
Volume 100 August 1992 301–339

with a molecular mass of ~100,000, also named capnophorin (Wieth and Bjerrum, 1983). The transport process at neutral pH can be described by ping-pong kinetics (Gunn and Fröhlich, 1979). This indicates that the transport protein is stable in at least two distinct conformations, one (S_i) having the empty anion binding site facing inward and the other (S_o) allowing anion binding from the exofacial side.

Studies of chloride translocation at alkaline pH_o by Wieth and Bjerrum (1982) demonstrated that positively charged groups with an apparent pK of 12 ($[Cl_o] = [Cl_i] = 165$ mM, 0°C) could be part of the exofacial binding site region, since the apparent pK of these groups (pK_{ts}) decreased when $[Cl_o]$ was reduced. To explain the stimulation of anion transport at alkaline pH_o, it was proposed that accessory binding groups that have a pK, pK_{ms} of ~11 stimulate anion translocation when deprotonated. Since stimulation of anion translocation was seen together with reduction in inhibitor binding, it was further assumed that the accessory groups were identical with the proposed modifier sites described by Dalmark (1976).

The types of amino acid residues involved in the titration process were examined by chemical modification from the exofacial side of the membrane using the arginine-modifying reagent phenylglyoxal (Wieth, Andersen, Brahm, Bjerrum, and Borders, 1982*a*; Wieth, Bjerrum, and Borders, 1982*b*). The pH dependency and the inactivation of the essential groups with phenylglyoxal depend on the $[Cl_o]$ in a manner that qualitatively parallels the change in pK of the titratable transport groups. Based on this observation, the chloride-sensitive groups with an apparent pK of 12 likely to be arginyl residues. Further support for the occurrence of essential arginine in the exofacial anion binding region was obtained by Bjerrum, Wieth, and Borders (1983).

Despite strong evidence for identity between the titratable groups and the modified arginyl residues and their involvement in binding/translocation of monovalent anions, Wieth and Bjerrum (1982) found no recruitment effects (change in apparent pK) when the chloride gradient across the membrane was altered by a change in $[Cl_i]$ with constant $[Cl_o]$. A recruiting effect should be observed if the system obeys ping-pong kinetics and the groups are directly involved in binding and/or translocation of the monovalent anions. Since the pK dependence on $[Cl_o]$ and $[I_o]$ was not found to fit a substrate binding site transport model, an interfacial potential transport model was proposed instead (Wieth and Bjerrum, 1982). It was conjectured that the positively charged groups could function as anion recognition sites guiding the anions to the transport site.

In this paper a new interpretation of the titration data is presented. The new model is founded on more recent experiments (Bjerrum, 1989*b*), showing that a recruitment effect can be observed if larger variations in the chloride gradient across the membrane are used, and if intra- and extracellular ionic strength are kept constant. Furthermore, the identity (proposed by Wieth and Bjerrum, 1982) of the pK_{ms} group (with an apparent pK of 11) and the halide modifier group has been disproved (Knauf and Mann, 1986). It was demonstrated that the self-inhibitory chloride binding site is located at the intracellular side of the membrane. This observation is of essential importance because the Wieth and Bjerrum (1982) definition for the theoretical pK_{ts} values (the values are model dependent) is inconsistent if the chloride self-inhibition modifier site and the pK_{ms} site are located

on opposite sides of the membrane. The apparent increase in the theoretical pk_{ts} with $[Cl_o]$, which completely disappeared at $[Cl_o] > 165$ mM, was a strong argument against the deprotonatable groups being part of the transport site.

When the data from Wieth and Bjerrum (1982) and the data presented here are reinterpreted in relation to the new model, a nearly linear increase is obtained for the theoretical apparent extracellular alkaline pK (pK_{alk}) as a function of log $[Cl_o]$. This relationship does not contradict that the involved groups are part of the exofacial transport site. The extracellular titration curves in the new model are explained on the basis of deprotonation of two positively charged groups which constitute essential parts of the exofacial anion binding site. The two deprotonatable groups appear to show mutual electrostatic interaction, with the pK of the groups changing when an anion is bound. Deprotonation of the first group converts the anion transport system into an alkaline state, which also displays ping-pong kinetics but with different kinetic parameters. Deprotonation of the second group blocks the transport of anions. The stimulation of transport at high pH_o is a simple consequence of the model, which is also capable of explaining the changes in chloride self-exchange as a function of pH_o when extracellular iodide inhibition is also included.

MATERIALS AND METHODS

Radioactive Isotopes and Chemical Reagents

^{36}Cl as sodium chloride, sp. act. 500 μCi/mmol, was obtained from AEK (Risø, Denmark); [^{3}H]inulin, sp.act. 900 mCi/mmol, was from the Radiochemical Centre (Amersham, UK).

All media were prepared from reagent grade chemicals. The buffers Tris (2-amino-2-hydroxymethyl-1,3-propanediol), TES (*N*-tris(hydroxymethyl)methyl-2-aminoethanesulfonic acid), CHES (2-(*N*-cyclohexylamino)ethanesulfonic acid), and CAPS (3-(*N*-cyclohexylamino)-1-propanesulfonic acid) were from Calbiochem Corp. (La Jolla, CA).

Preparation of Resealed Ghosts

Intact red blood cells (RBC) and ordinary resealed ghosts containing 165 mM KCl, 2 mM Tris, and 0.5 mM EGTA/EDTA were prepared as described by Bjerrum et al. (1983).

Citrate-containing resealed ghosts were prepared from whole blood from healthy donors stabilized with either heparin or EDTA. After removal of the plasma and buffy coat the blood was washed three times with 165 mM KCl and packed to 80% cytocrit, determined from the extracellular inulin space (Funder and Wieth, 1976). The blood cells (5–10 ml) were hemolyzed in 200 ml 20 mM potassium citrate/citric acid and 1.3 mM magnesium citrate (pH 6.0 at 0°C). The hemolyzed suspension of red cells, which in some preparations also contained sucrose, had a pH of ~6.5. The suspension was incubated for 5 min at 0°C before adding 20 ml of reversal solution containing 25 mM Tris and an amount of KCl to give the desired final [Cl] in the suspension. In the absence of KCl in the reversal solution a $[Cl_i]$ of 3–5 mM was obtained. The reversal solution was adjusted with KOH to give a pH in the cell suspension of 7.2 at 0°C. The hemolyzed cells resealed at 38°C for 45 min were washed three times in 25 mM potassium citrate, *X* mM KCl, and 1 mM potassium phosphate. The final $[Cl_i]$ was determined from the distribution ratio for ^{36}Cl between the intracellular and extracellular phases (as described by Wieth and Bjerrum, 1982), taking into account the 1–2 mM chloride added with the ^{36}Cl. The ^{36}Cl-labeled ghosts packed for efflux experiments in nylon tubes as described by Funder and Wieth (1976) had an extracellular trapped volume of ~8% estimated from the insulin space.

Ghosts with low $[Cl_i]$ = 16.5 in high $[Cl_o]$ = 165 mM were obtained by hemolysis of 1 vol ice-cold 50% suspension of RBC in 20 vol 4 mM magnesium sulfate, 3.8 mM acetic acid, and 120 mM sucrose (pH 3.4–3.6, 0°C), followed by addition of 1 vol resealing solution containing 25 mM Tris and 1 M sucrose (pH 10.5, 0°C). The ghosts in the suspension (having a pH of ~7.2), after incubation at 38°C for 45 min, were washed twice in 16 mM KCl, 270 mM sucrose, and 2 mM phosphate buffer (pH 7.3, 0°C), and once in the same medium without phosphate buffer, before addition of ^{36}Cl and packing for the efflux experiment.

Electrolyte Media

The efflux experiments with ordinary resealed ghosts initially containing 165 mM KCl, pH 7.3, were carried out in mixtures of 165 mM KCl and 25 mM potassium citrate, 200 mM sucrose. These media are isotonic with, and have approximately the same ionic strength as, the 165 mM KCl medium.

The ordinary type of ghosts were also used in experiments employing higher $[Cl_i]$. These experiments were performed by measuring the efflux in media with higher $[Cl_o]$. Since resealed ghosts behave as almost perfect osmometers with a constant membrane area, $[Cl_i]$ increases to the same concentration as the $[Cl_o]$ as the ghosts shrink. The volume of these ghosts, which initially contained ~2% hemoglobin, was corrected for the increase in hemoglobin dry weight when shrunken.

The measurements of the efflux from resealed citrate ghosts were performed under conditions of intra- and extracellular ionic strength corresponding to ~150 mM KCl, except in the experiments of Fig. 8, where the intracellular ionic strength was increased when $[Cl_i]$ was increased by shrinkage of the ghosts. The citrate ghosts, which initially contained 16 mM KCl, 25 mM potassium citrate, and 20 mM sucrose, were shrunken to an intracellular concentration of maximally 66 mM KCl by suspension in hypertonic media composed of KCl, sucrose, and potassium citrate, taking into account the osmotic coefficients (Weast, 1987), to give the desired $[Cl_i]$ and $[Cl_o]$.

Buffering of the Media

To avoid influence from buffer ions, as little as possible extracellular buffer was used in the different experiments. The buffer system used to maintain constant pH_o was 0.5 mM phosphate and 0.5 mM CHES unless otherwise indicated. To avoid influence from atmospheric CO_2, the media were freshly prepared at neutral pH and titrated to the desired alkaline pH_o immediately before measuring the ^{36}Cl efflux. The use of buffers was found to be necessary only at pH values between 8 and 10.5. At higher pH values the $[OH^-]$ is sufficient to keep pH constant during the experiment (Wieth and Bjerrum, 1982). The pH change observed on addition of ghosts to the efflux medium never exceeded 0.1 pH unit in any experiment.

To ensure precise measurements at alkaline pH_o, glass electrodes (G202 B or C) and calomel electrode K401 (chosen to have a minimum diffusion potential; Radiometer, Copenhagen, Denmark) were calibrated at 0°C with certified National Bureau of Standards buffers: i.e., sodium phosphate buffers (pH 6.98 and 7.53) and 0.01 M sodium tetraborate buffer (pH 9.46). The glass as well as the calomel electrodes were cleaned regularly with protein remover (Cleaning Solution S5332; Radiometer) to avoid development of diffusion potentials due to lipid and protein deposits.

Determination of the Chloride Self-Exchange Efflux

The rate coefficient (k) for chloride self-exchange and the chloride efflux per unit membrane area (J) were obtained as described by Wieth and Bjerrum (1982), except in experiments were F (the fraction of extracellular chloride [m_o] divided by the total amount of chloride in the

system [$m_o + m_i$]) were below ~0.95. In that case the increase in activity in ^{36}Cl in the medium at steady-state conditions is described by the equation:

$$\{1 - [a_t/(F \cdot a_s)]\} = \{1 - [a_0/(F \cdot a_s)]\} \cdot e^{-F \cdot k \cdot t} \quad \text{(M1a)}$$

or

$$a_t = F \cdot a_s \cdot \langle 1 - \{1 - [a_0/(F \cdot a_s)]\} \cdot e^{-F \cdot k \cdot t} \rangle \quad \text{(M1b)}$$

where a_0 and a_t are the radioactivity in the extracellular medium at times 0 and t, respectively, a_s is the ^{36}Cl activity in a sample of the ghost efflux suspension, and k is the rate coefficient. The factor F was determined separately from S_v (the volume of the efflux suspension), a_s, [Cl_o] (in the efflux medium), R ([^{36}Cl] distribution ratio between the intracellular and extracellular phases of the packed ghost), G_{ac} (^{36}Cl activity per milligram packed ghosts), [Cl_o^p] (the [Cl] in the extracellular water phase between the packed ghosts), W (the fractional water content per milligram packed ghosts), and I_{sp} (inulin space, the trapped volume per milligram packed ghosts), using the equation:

$$F = m_o/(m_o + m_i) = [S_v \cdot [Cl_o] + (S_v \cdot a_s/G_{ac}) \cdot I_{sp} \cdot [Cl_o^p]]/[S_v \cdot [Cl_o] + (S_v \cdot a_s/G_{ac}) \cdot (I_{sp} \cdot [Cl_o^p] + (W - I_{sp}) \cdot R \cdot [Cl_o^p])] \quad \text{(M2)}$$

The apparent rate coefficient for chloride efflux, $k' = F \cdot k$, as well as the percentage of intracellular ^{36}Cl activity at time 0 $\{1 - [a_0/(F \cdot a_s)]\}$ was obtained (after determination of the F value) by linear regression of a plot of $\ln\{1 - [a_t/(F \cdot a_s)]\}$ vs. time (Eq. M1a) or by direct nonlinear fit to Eq. M1b using the Enzfitter program (see below). The two methods gave nearly identical results. The chloride efflux per unit membrane area was calculated as described by Funder and Wieth (1976) with the value for k determined as k'/F.

Nonlinear Regression

Nonlinear regression fits to the various equations (using simple weighting, unless otherwise indicated) were performed with the Enzfitter data analysis program written for the IBM PC by R. J. Leatherbarrow (Elsevier-BIOSOFT, Cambridge, UK).

THEORY

The presented model for extracellular titration of the anion transport function involves two positively charged deprotonatable groups located in the exofacial anion binding site. It is assumed that one of the groups deprotonates first (either due to the local position in the protein or due to the intrinsic pK of the group), and that this deprotonation changes the transport system from a transporting state (a) at neutral pH to a transporting state (b) at alkaline pH. Both states are assumed to exhibit ping-pong kinetics, but the kinetic parameters such as chloride affinity and maximal transport rate are different. The transport process is halted when the second group (the group with the higher pK) is also deprotonated. It is assumed, moreover, that both groups cannot be protonated/deprotonated from the intracellular side of the membrane (see Discussion).

The equation for transport with a deprotonatable transport site at alkaline pH_o was evolved from the homo-exchange ping-pong equation (at neutral pH) without rate-limiting step restrictions (Knauf, Law, Tarshis, and Furuya, 1984; Fröhlich and Gunn, 1986). The equation was analyzed assuming that the translocation steps are

very slow compared with the off and on rates involved in binding on the two sides. The efflux (J) under this condition was found to be equal to the theoretical maximal obtainable efflux (J_{max}) multiplied by the sum of the concentrations of the loaded intracellular and extracellular transporting conformations ($[S_iCl_i] + [S_oCl_o]$) divided by the total concentration of all conformational forms, which is equal to the total concentration of transport protein molecules. In a simple ping-pong system without acid/base titration of the transport sites, self-inhibition, or competitive inhibition from other anions the transport efflux equation becomes:

$$J = J_{max} \cdot \{[S_oCl_o] + [S_iCl_i]\} / \{[S_oCl_o] + [S_iCl_i] + [S_o] + [S_i]\} \quad \text{(T1)}$$

where J_{max} is the maximal efflux, and $[S_o]$ and $[S_i]$ are the concentrations of unloaded forms, respectively.

When more than one transport conformation can undergo translocation, the total efflux will be the sum of the effluxes for the two transport routes (a) and (b):

$$J = J^a_{max} \cdot \{([S^a_oCl_o] + [S^a_iCl_i])/[S_t])\} + J^b_{max} \cdot \{([S^b_oCl_o] + [S^b_iCl_i])/[S_t]\} \quad \text{(T2)}$$

where $[S_t]$ is the total concentration of transporter molecules, as stated above. This equation can also be expressed as:

$$J = J^a_{max} \cdot \{([S^a_oCl_o] + [S^a_iCl_i] + (J^b_{max}/J^a_{max}) \cdot (S^b_oCl_o] + [S^b_iCl_i])\}/[S_t] \quad \text{(T3)}$$

The Transport Model Equations with Deprotonatable Extracellular Sites

A schematic presentation of the different conformations involved in the proposed model, which also includes chloride self-inhibition and inhibition with I_o, is shown in Fig. 1. It is assumed that the chloride self-inhibition takes place from the intracellular side (Knauf and Mann, 1986) with the same constant (K_m) at neutral and alkaline pH_o (because pH_i stays constant in all experiments) and indiscriminately hinders both the forward and backward translocation. Since the inhibition is only noticeable at high $[Cl_i]$, with nearly saturation of the substrate binding site, modifier effects on the unloaded transport sites have been ignored for the sake of simplicity (see Discussion).

The concentrations of the possible conformational states (in Fig. 1), determined from the law of mass action in relation to the $[S_oH]$, are defined in Table I. When these concentrations are substituted into Eq. T3, $[S_oH]$ vanishes because it is a factor in all terms. If the effects of iodide are omitted, and the terms multiplied by $K_4/([H_o] \cdot [Cl_o])$, the equation can be rearranged to:

$$J = \frac{J^a_{max} \cdot \{(1 + K^a_{ex})/K_o) + (J^b_{max}/J^a_{max}) \cdot (K_4/[H_o]) \cdot (1 + K^b_{ex})/K'_o\}}{\begin{array}{l}\{(((K^a_{ex} + 1)/K_o) + (K_4/[H_o]) \cdot (K^b_{ex} + 1)/K'_o)) \cdot (1 + ([Cl_i]/K_m))\} \\ + \{(K_i \cdot K^a_{ex}/(K_o \cdot [Cl_i])) + (K_4/[H_o]) \cdot (K'_i \cdot K^b_{ex}/(K'_o \cdot [Cl_i]))\} \\ + \{((K_4/[H_o]) \cdot ((K_5/[H_o]) + 1) + 1)/[Cl_o]\}\end{array} \quad \text{(T4)}$$

A simple ping-pong system is characterized by an asymmetry factor and a half-saturation constant with $[Cl_o] = [Cl_i]$ (Knauf and Mann, 1984). The (a) system presented here is defined by the asymmetry factor $A^a = K^a_{ex} \cdot K_i/K_o$ and the apparent half-saturation constant $K^a_{Cl} = (K_i \cdot K^a_{ex} + K_o)/(1 + K^a_{ex})$, where K^a_{ex} is defined as $k'/k =$

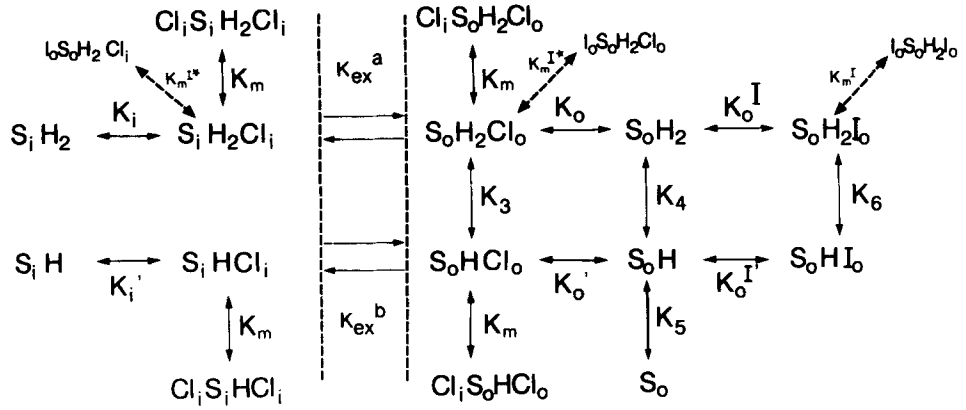

FIGURE 1. The reaction scheme for the proposed model. The constants K_{ex}^a and K_{ex}^b are defined as $k^{a\prime}/k^a = [S_iH_2Cl_i]/[S_oH_2Cl_o]$ and $k^{b\prime}/k^b = [S_iHCl_i]/[S_oHCl_o]$, respectively, at steady-state conditions.

$[S_iH_2Cl_i]/[S_oH_2Cl_o]$ and K_i and K_o are the intrinsic intracellular and extracellular dissociation constants, respectively. From these relations the following general equation can be established:

$$(1 + K_{ex})/K_o = (A + 1)/K_{Cl} \qquad \text{(T5)}$$

Substitution of this equation and the definition for the asymmetry factor into Eq. T4

TABLE I

The Different Model Terms, Defined in Relation to $[S_oH] = [T]$ in Accordance with the Law of Mass Action

$[S_o] = [T]\cdot K_5/[H_o]$
$[S_oH] = [T]\cdot 1$
$[S_oH_2] = [T]\cdot[H_o]/K_4$
$[S_oHCl_o] = [T]\cdot[Cl_o]/K_o'$
$[S_oH_2Cl_o] = [T]\cdot[H_o]\cdot[Cl_o]/(K_4\cdot K_o) = [T]\cdot[H_o]\cdot[Cl_o]/(K_o'\cdot K_2)$
$[S_iH_o] = [T]\cdot[Cl_o]\cdot K_{ex}^b\cdot[Cl_i]/(K_o'\cdot K_i')$
$[S_iH_2] = [T]\cdot[H_o]\cdot[Cl_o]\cdot K_{ex}^a\cdot[Cl_i]/(K_4\cdot K_o\cdot K_i)$
$[S_iHCl_i] = [T]\cdot[Cl_o]\cdot K_{ex}^b/K_o'$
$[S_iH_2Cl_i] = [T]\cdot[H_o]\cdot[Cl_o]\cdot K_{ex}^a/(K_4\cdot K_o)$

Intracellular chloride modifier terms:
$[Cl_iSHCl_o] = [T]\cdot[Cl_o]\cdot[Cl_i]/(K_o'\cdot K_m)$
$[Cl_iSHCl_i] = [T]\cdot[Cl_o]\cdot K_{ex}^b\cdot[Cl_i]/(K_o'\cdot K_m)$
$[Cl_iSH_2Cl_o] = [T]\cdot[H_o]\cdot[Cl_o]\cdot[Cl_i]/(K_4\cdot K_o\cdot K_m)$
$[Cl_iSH_2Cl_i] = [T]\cdot[H_o]\cdot[Cl_o]\cdot K_{ex}^a\cdot[Cl_i]/(K_4\cdot K_o\cdot K_m)$

Iodide binding terms:
$[S_oHI_o] = [T]\cdot[I_o]/K_o^{I'}$
$[S_oH_2I_o] = [T]\cdot[H_o]\cdot[I_o]/(K_4\cdot K_o^I)$
$[I_oS_oH_2I_o] = [T]\cdot[H_o]\cdot[I_o]^2/(K_4\cdot K_o^I\cdot K_m^I)$
$[I_oS_oH_2Cl_o] = [T]\cdot[H_o]\cdot[Cl_o]\cdot[I_o]/(K_4\cdot K_o\cdot K_m^{I*})$
$[I_oS_iH_2Cl_i] = [T]\cdot[H_o]\cdot[Cl_o]\cdot K_{ex}^a\cdot[I_o]/(K_4\cdot K_o\cdot K_m^{I*})$

for transport system (a) and (b), respectively, gives:

$$J = \frac{J^a_{max}\cdot\{((A^a + 1)/K^a_{Cl}) + D\cdot(K_4/[H_o])\cdot(A^b + 1)/K^b_{Cl}\}}{\{((K_4/[H_o])\cdot((A^b + 1)/K^b_{Cl}) + ((A^a + 1)/K^a_{Cl}))\cdot(1 + ([Cl_i]/K_m))\} + \{((K_4/[H_o])\cdot((K_5/[H_o]) + 1) + 1)/[Cl_o]\} + \{(A^a/[Cl_i]) + (K_4/[H_o])\cdot(A^b/[Cl_i])\}} \quad \text{(T6)}$$

where A^a and A^b are the asymmetry factors and K^a_{Cl} and K^b_{Cl} the half-saturation constants for chloride measured under conditions where $[Cl_o] = [Cl_i]$) for the (a) neutral and (b) alkaline transport system respectively, and D is the ratio J^b_{max}/J^a_{max}. Eq. T6 contains only transport constants which can be determined experimentally, as explained below.

Determination of the Parameters at Neutral pH_o (pH 8)

At neutral pH_i and pH_o the transport via the (b) system can be neglected, and Eq. T6 simplifies to:

$$J = J^a_{max}\cdot\{(A^a + 1)/K^a_{Cl}\}/\{((A^a + 1)/K^a_{Cl})\cdot(1 + ([Cl_i]/K_m)) + (A^a/[Cl_i]) + (1/[Cl_o])\} \quad \text{(T7)}$$

When $[Cl_o] = [Cl_i]$, Eq. T7 can be rearranged to the form of a simple Michaelis-Menten equation including a modifier term, after dividing the numerator and denominator by $(A^a + 1)$:

$$J = J^a_{max}\cdot[Cl]/\{K^a_{Cl} + [Cl]\cdot(1 + ([Cl_i]/K_m))\} \quad \text{(T8)}$$

The three parameters V^a_{max}, K^a_{Cl}, and K_m can therefore be determined by simple nonlinear fitting to a plot of chloride self-exchange vs. [Cl] at pH_o 8. Knowing K^a_{Cl} and K_m, A^a can, for example, be determined by a simple nonlinear fit to a plot of chloride self-exchange vs. $[Cl_o]$ using Eq. T7.

Determination of pK for the First Deprotonatable Group

At pH_o values close to pK_4, at neutral pH_i, and at low $[Cl_o]$ and with the assumption that $pK_4 \ll pK_5$ and that $K_o \ll K'_o$, the S_o and the S_oHCl_o terms can both be neglected. As a consequence of the negligible S_oHCl fraction, the transport via the alkaline system can also be neglected and the approximative transport equation with these conditions becomes:

$$J = J^a_{max}\cdot\{(A^a + 1)/K^a_{Cl}\}/\{((1 + (K_4/[H_o]))/[Cl_o]) + ((A^a + 1)/K^a_{Cl})\cdot(1 + ([Cl_i]/K_m)) + (A^a/[Cl_i])\} \quad \text{(T9)}$$

If titration is performed at constant $[Cl_i]$ and $[Cl_o]$ the equation has the same form as a simple titration equation:

$$J = J^{app}_{max}\cdot 10^{-pH_o}/(10^{-pKapp} + 10^{-pH_o}) \quad \text{(T9a)}$$

or

$$1/J = (1/[H_o])\cdot(10^{-pKapp}/J^{app}_{max}) + 1/J^{app}_{max} \quad \text{(T9b)}$$

where $10^{-pK_{app}} = K_4/\{((A^a + 1)\cdot[Cl_o]/K^a_{Cl})\cdot(1 + ([Cl_i]/K_m)) + A^a\cdot([Cl_o]/[Cl_i]) + 1\}$ and J^{app}_{max} is equal to J in Eq. T9 with $[H_o] = \infty$. A plot of $1/J$ vs. $1/H_o$ should therefore be a straight line for measurements made at a constant low $[Cl_o]$ and in a narrow interval below and around pK_4. If the relation is examined at different low $[Cl_o]$, lines should be obtained which intersect to the left of the ordinate. The abscissa value of the intersection (defined from $J_1 = J_2$ at two different $[Cl_o]$) is found from Eq. T9 to represent the negative value of $1/K_4$. This type of analysis has recently been described by Fröhlich and Gunn (1986), and by Knauf, Mann, Kalwas, Spinelli, and Ramjeesingh (1987).

Determination of pK for the Second Deprotonatable Group

At high pH_o (≥ 11.6) the transport equation (Eq. T6) can be simplified since the transport via the (a) transport system can be neglected:

$$J = J^b_{max}\cdot(A^b + 1)/K^b_{Cl}/\{(((K_5/[H_o]) + 1)/[Cl_o]) + ((A^b + 1)/K^b_{Cl})\cdot(1 + ([Cl_i]/K_m)) + (A^b/[Cl_i])\} \quad (T10)$$

This equation has a mathematical form similar to Eq. T9 used for determination of K_4. The K_5 value can therefore be determined (at $pH_o > 11.6$) from the intersection of the lines obtained from plots of $1/J$ vs. $1/[H_o]$ at various $[Cl_o]$.

Determination of $D = J^b_{max}/J^a_{max}$

An approximate value of $D = J^b_{max}/J^a_{max}$ can be obtained at high $[Cl_i]$ as the ratio $J^{app\ pH_o12}_{max}/J^{app\ pH_o8}_{max}$ as explained below. This ratio determined from Eqs. T10 and T7 gives:

$$J^{app\ pH_o12}_{max}/J^{app\ pH_o8}_{max} = \{J^b_{max}/J^a_{max}\}\cdot\{1 + ([Cl_i]/K_m) + K^a_{Cl}\cdot A^a/([Cl_i]\cdot(A^a + 1))\}/\{1 + ([Cl_i]/K_m) + K^b_{Cl}\cdot A^b/([Cl_i]\cdot(A^b + 1))\} = \{J^b_{max}/J^a_{max}\}\cdot F_D \quad (T11)$$

where $F_D = \{1 + ([Cl_i]/K_m) + (K^a_{Cl}\cdot A^a/[Cl_i]\cdot(A^a + 1))\}/\{1 + ([Cl_i]/K_m) + (K^b_{Cl}\cdot A^b/[Cl_i]\cdot(A^b + 1))\}$. When $Cl_i \rightarrow \infty$, $F_D \rightarrow 1$ and thus $J^{app\ pH_o12}_{max}/J^{app\ pH_o8}_{max} \rightarrow J^b_{max}/J^a_{max}$.

The value of D thus represents approximately the ratio between the intercepts with the ordinate of plots of $1/J$ vs. $1/[Cl_o]$ (with the same high $[Cl_i] = 330$ mM) obtained at pH_o 12 and pH_o 8, respectively.

Determination of the Asymmetry Factors A^b and K^b_{Cl}

At $[Cl_i] < 70$ mM, the intracellular modifier effect (with a K_m of ~ 450 mM) can be neglected. With $[Cl_o] = [Cl_i]$ the self-exchange flux equation at $pH_o \geq 11.6$, derived from Eq. T10, becomes:

$$J = J^b_{max}\cdot\{(A^b + 1)/K^b_{Cl}\}/\{(((K_5/[H_o]) + A^b + 1)/[Cl]) + ((A^b + 1)/K^b_{Cl})\} \quad (T12)$$

The K^b_{Cl} constants of this equation cannot directly be determined from reduction to a simple Michaelis-Menten equation (the method used for determination of K^a_{Cl}) due to the term $K_5/[H_o]$. K^b_{Cl} and A^b were therefore determined by another method. Eq. T12

was reduced to:

$$J = [Cl]/(S_1 + ([Cl]/J^b_{max})) \quad \text{(T12a)}$$

where $S_1 = \{(K_5/[H_o]) + A^b + 1\}/\{J^b_{max}\cdot(A^b + 1)/K^b_{Cl}\}$. The general equation for alkaline self-exchange when the intracellular modifier effect is neglected (derived from Eq. T10) is written:

$$J = J^b_{max}\cdot\{(A^b + 1)/K^b_{Cl}\}/\{((K_5/[H_o]) + 1)/[Cl_o]) + ((A^b + 1)/K^b_{Cl}) + (A^b/[Cl_i])\} \quad \text{(T13)}$$

This equation reduces at constant $[Cl_o]$ and at $pH_o \geq 11.6$ to:

$$J = [Cl_i]/\{S_2 + ([Cl_i]/J^{app}_{max})\} \quad \text{(T13a)}$$

where $J^{app}_{max} = J^b_{max}/\{((1 + (K_5/[H_o])) + 1)\cdot K^b_{Cl}/([Cl_o]\cdot(A^b + 1))\}$ and $S_2 = A^b/\{J^b_{max}\cdot(A^b + 1)/K^b_{Cl}\}$. A^b can be determined from the value for K_5 (which has already been obtained) and the ratio between S_1 and S_2 (both having the same denominator) by:

$$S_1/S_2 = \{A^b + (K_5/[H_o]) + 1\}A^b \rightarrow A^b = \{(K_5/[H_o]) + 1\}/((S_1/S_2) - 1) \quad \text{(T13b)}$$

Knowing A^b, the value of K^b_{Cl} can be obtained from any other measurements of chloride self-exchange as a function of $[Cl_o]$ performed at high pH_o by a simple nonlinear fit to Eq. T10 using the previously determined constants A^a, K_5, and K_m.

Determination of the Iodide Binding Constants

Extracellular iodide (I_o) inhibition is also considered. It is assumed that I_o binds competitively with Cl_o to the binding forms S_oH_2 and S_oH, as well as to an extracellular modifier site with the binding constants K^I_o, K^I_o, and K^I_m, respectively (see Fig. 1). A possible competition between I_o and Cl_o at the extracellular modifier site at neutral pH_o is neglected because the Cl_o affinity appears to be much lower than the I_o affinity (Knauf and Mann, 1986). Since I_o modifier inhibition at alkaline pH_o (if existing) is expected to decrease (due to awaited deprotonation of positively charged groups at the modifier binding site) and thus be of minor influence on the model constants, the corresponding binding terms have also been ignored. The quantitative effects of this omission are dealt with in the Results. Since modifier inhibition at $pH_o \sim 8$ is only noticeable at high I_o, it is moreover assumed that the I_o modifier binding at neutral pH_o only takes place with an anion bound at the substrate binding site. This inhibition is assumed to involve the same modifier binding constant (K^I_m) independent of whether the transport site is saturated with I_o or Cl_o. This assumption is justified by a quantitative examination in the Results of the importance of the $K^{I^*}_m$ (the iodide inhibitor constant with chloride on the transport site). When the iodide inhibitor constants (see Fig. 1 and Table I) are included in Eq. T6, this equation becomes:

$$J = \frac{J^a_{max}\cdot\{((A^a + 1)/K^a_{Cl}) + D\cdot(K_4/[H_o])\cdot(A^b + 1)/K^b_{Cl}\}}{\begin{aligned}&\{((A^a + 1)/K^a_{Cl})\cdot(1 + ([Cl_i]/K_m) + ([I_o]/K^{I^*}_m))\}\\ &+ \{(K_4/[H_o])\cdot((A^b + 1)/K^b_{Cl})\cdot(1 + ([Cl_i]/K_m))\}\\ &+ \{(K_4/[H_o])\cdot((K_5/[H_o]) + ([I_o]/K^{I'}_o) + 1)/[Cl_o]\}\\ &+ \{(([I_o]/K^I_o)\cdot(1 + ([I_o]/K^I_m)) + 1)/[Cl_o]\}\\ &+ \{(A^a/[Cl_i]) + (K_4/[H_o])\cdot(A^b/[Cl_i])\}\end{aligned}} \quad \text{(T14)}$$

The values for K_o^I, $K_o^{I'}$, and J_{max}^a were determined by direct nonlinear fit to plots of J vs. pH_o at constant $[Cl_o]$, $[Cl_i]$, and $[I_o]$, using the values for the other transport parameters already determined. The value of K_m^I (the I_o self-inhibitor constant) was determined at pH_o 8 and constant Cl_o and Cl_i, from a normalized plot of the ^{36}Cl efflux vs. $[I_o]$ by nonlinear regression to:

$$J/J_{I=0} = 1/\{(I_o/K_o^{I\,app})\cdot(1 + (I_o/K_m^I)) + 1\} \quad \text{(T15)}$$

This equation was derived from Eq. T14 by omission of all alkaline terms, rearrangement, and collection of the constant terms (different from the K_m^I-containing term) in $K_o^{I\,app}$.

RESULTS

Effects of Ionic Strength on the Titration

The experiments were designed such that the chloride self-exchange flux was measured as a function of pH_o, $[Cl_o]$, and $[Cl_i]$, keeping the initial pH_i constant at pH 7.3. The experiments were carried out at a constant ionic strength corresponding to ~150 mM KCl whenever possible. Potassium citrate was chosen as being most suitable for use as a substitute for chloride when the [Cl] was reduced on both the sides of the membrane. It has a high ionic strength contribution and shows only slight inhibition of chloride transport at $8 < pH_o < 9$ (cf. Fig. 2 *A*) (Wieth and Bjerrum, 1982). A constant ionic strength was selected primarily because the apparent transport pK was very sensitive to this parameter (Fig. 2), but also because resealed ghosts are more stable in a sucrose/citrate medium of low [Cl] than in a corresponding medium lacking citrate.

The apparent pK for transport inactivation at low ionic strength and $[Cl_o] = 5$ mM (Fig. 2 *A*) is displaced 0.35 pH units to the right when the ionic strength of the medium is raised with citrate. Besides this effect the presence of citrate also stimulates chloride self-exchange (the crossing over of the curves in Fig. 2 *A*). The effect (analyzed in the Discussion) appears mainly to reflect an influence of free citrate ions on the titratable groups rather than a competitive inhibition at the binding site. The effect is less pronounced at higher chloride (0.2 pH units at 16 mM $[Cl_o]$) (Fig. 2 *B*) and more pronounced at lower $[Cl_o]$ (0.5 pH units at 1.8 mM $[Cl_o]$) (Fig. 2 *C*) and can, at infinite dilution, be estimated to be ~0.7 pH units when the ionic strength is changed from 0 to 150 mM. The experiment with 1.8 mM $[Cl_o]$ with sucrose substitution (Fig. 2 *C*) was performed on intact RBC, since resealed ghosts are unstable at low $[Cl_o]$.

Determination of the Transport Parameters at Neutral pH

The half-saturation constant for chloride binding, K_{Cl}^a, the intracellular chloride self-inhibition constant, K_m, and J_{max}^a were determined with $[Cl_i] = [Cl_o]$ and pH_o 8, by nonlinear fit of the transport data in Fig. 3 to Eq. T8. J_{max}^a was found to be 445 (SD 20) pmol $cm^{-2}\,s^{-1}$, K_{Cl}^a 29.5 (SD 3.1) mM, and K_m 452 (SD 73) mM. Knowing the values of K_{Cl}^a and K_m, the asymmetry factor A^a and J_{max}^a were determined from the data of Fig. 4. A direct nonlinear fit of the data (at pH_o 8 and $[Cl_i] = 165$ mM) to Eq. T7 gave the following values $A^a = 10.7$ (SD 1.3) and $J_{max}^a = 457$ (SD 8) pmol $cm^{-2}\,s^{-1}$, respectively. K_o^{app} and J_{max}^{app} were further obtained from the same set of data but

with a nonlinear fit to simple Michaelis-Menten kinetics. K_o^{app} and J_{max}^{app} were found to be 1.64 (SD 0.18) mM and 299 (SD 5) pmol cm^{-2} s^{-1}, respectively.

Determination of pK of the First Deprotonatable Group

A plot (Fig. 5 *A*) of the chloride self-exchange efflux as a function of pH_o at $[Cl_o]$ = 10 was compared with the simple sigmoid titration function (Eq. T9a). The experi-

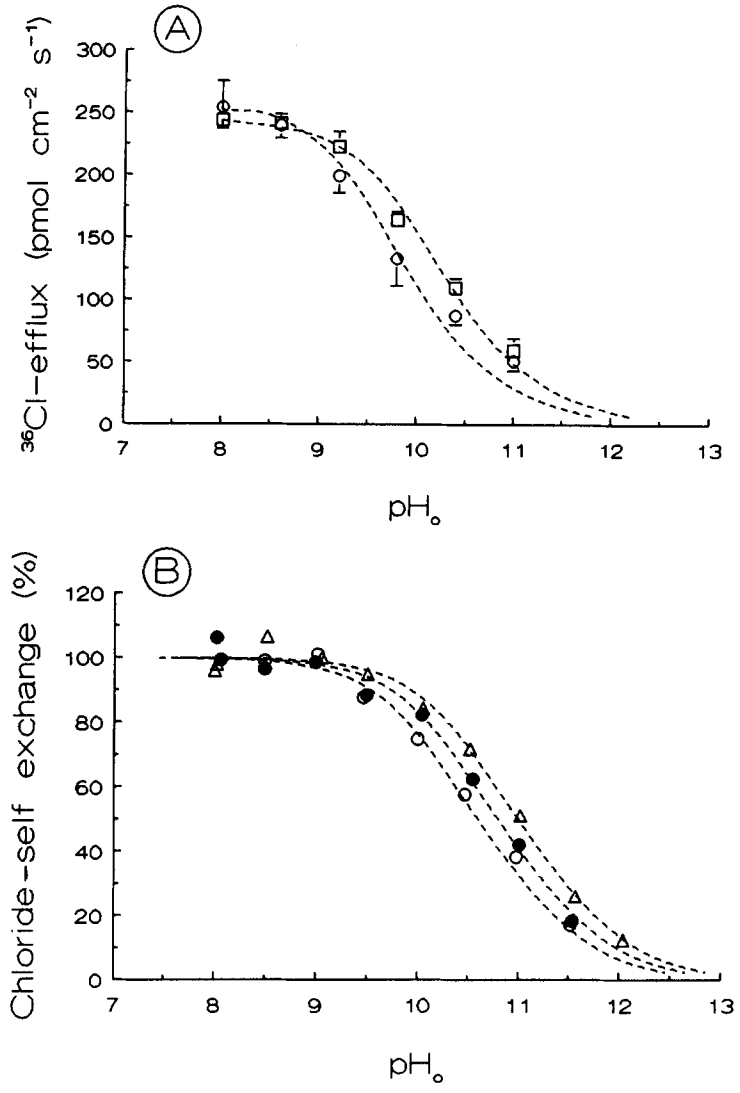

mental data do not follow a simple titration curve, but start to deviate from the simple curve at higher pH values, as expected if more than one titratable group is involved. A replot of the data (Fig. 5 *B*; $1/J$ plotted as a function of $1/[H_o]$) demonstrates a bending curve which appears to be asymptotically linear at both ends.

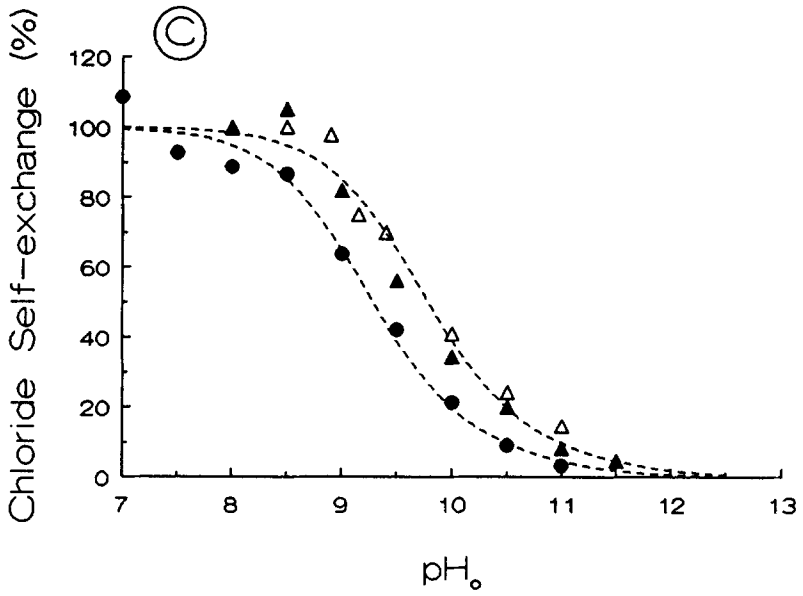

FIGURE 2. (*A*) Effects of extracellular ionic strength on ^{36}Cl efflux as a function of pH_o in resealed ghosts at $[Cl_o]$ = 5 mM, 0°C. Ghosts: initial pH_o 7.2, 165 mM KCl, 2 mM Tris. Media: substitution with isotonic sucrose (○); substitution with isotonic sucrose citrate (□). Buffer was 0.5 mM CHES and 0.5 mM phosphate (cf. Materials and Methods). The individual points are the mean fluxes of three sets of experiments (performed on different days), with the bars indicating SD. The apparent effect on pK on changing the ionic strength from ~5 to ~150 mM was ~0.35 pH units (from 9.8 to 10.15). (*B*) The effect of extracellular ionic strength on chloride self-exchange as a function of pH_o, $[Cl_o]$ = 16.5 mM. Ghosts: initial pH_o 7.3, 165 mM KCl, 2 mM Tris. Media: $[Cl_o]$ = 16.5 mM, Buffer: 0.5 mM CHES and 0.5 mM phosphate substituted to isotonicity with sucrose (○), citrate sucrose (●), and citrate (△) (cf. Materials and Methods). The experiments (○ and ●) were performed on two different days with resealed ghosts from the same donor. The magnitude of the chloride fluxes was calculated relative to the mean efflux values found at pH 8.0–8.5. These values correspond to 265 (○), 247 (●), and 236 pmol cm^{-2} s^{-1} (△), respectively. The apparent pK_o obtained from the data at $[Cl_o]$ = 16.5 mM and extracellular ionic strength corresponding to ~16.5 (○), ~155 (●), and ~640 mM (△) are ~10.6, 10.8, and 11.0, respectively. (*C*) Effect of ionic strength at very low $[Cl_o]$, 0°C. Resealed ghosts: initial intracellular pH 7.2, 165 mM KCl, 2 mM Tris. Medium: 1.8 mM KCl substituted with isotonic sucrose citrate (△). RBC: initial pH 7.2, 110 mM KCl. Medium: 1.8 mM KCl substituted with isotonic sucrose (●), or with sucrose citrate (▲). Buffer: 2 mM TES, 2 mM CHES, 2 mM CAPS. The magnitude of the chloride fluxes in the three experiments, all obtained on different days, is shown relative to the values (155, 231, and 187 pmol cm^{-2} s^{-1}). K_o^{app} for chloride binding to the RBC in the sucrose medium at pH 7.0 was ~0.45 mM, and in the sucrose citrate medium at pH 8.0 was ~1.2 mM. The apparent pK_o at an ionic strength corresponding to 1.8 mM (●) and 150 mM (▲, △) was ~9.2 and ~9.7, respectively.

The dotted straight line shows the relation between $1/J$ and $1/[H_o]$ as expected from Eq. T9b. The identity between the dotted line and the curve in the pH interval 8–9.7 indicates that K_4 can be determined in this interval. Data obtained in the narrow pH interval at four $[Cl_o]$'s equal to 1.3, 2.3, 4.2, and 10 mM are shown in Fig. 5 *C*. Plots of J vs. pH_o for the various $[Cl_o]$ were nonlinearly fitted to Eq. T9b and transformed

into the plot shown in Fig. 5 *C*. Since the efflux data at the different $[Cl_o]$'s were obtained on different days, all the data have been normalized. The chloride self-exchange fluxes obtained at one $[Cl_o]$ were divided by the value obtained at 165 mM KCl in the same experiment, and multiplied by the mean value for chloride self-exchange obtained at 165 mM $[Cl_o]$ in all four experiments. The four lines intersect to the left of the ordinate (close to the same point) at an abscissa value which, in accordance with Eq. T9, corresponds to $-1/K_4$. The intrinsic pK_4 value was

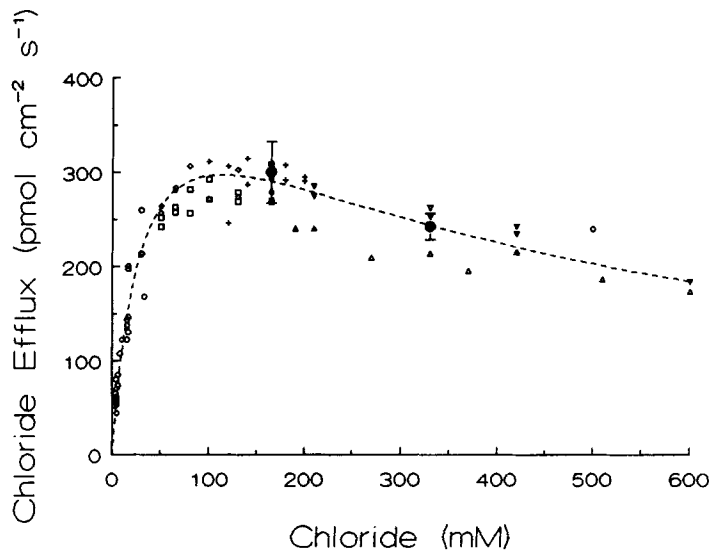

FIGURE 3. Chloride self-exchange of resealed ghosts ($[Cl_o] = [Cl_i]$) as a function of [Cl] at pH_o 8.0, 0°C. Determination of the half-saturation constant K^a_{Cl} and the constant for self-inhibition K_m. The points (○) show results obtained on different days with resealed ghosts prepared with different $[Cl_i]$. The data points (□, ◇, +, ▽, △) show different series of experiments. Each series was obtained by shrinkage of the ghosts in media with increasing [Cl] (cf. Materials and Methods). Ordinary resealed ghosts were prepared with 50 mM (□, ◇), 100 mM (+), and 165 mM (△, ▽) intracellular KCl, respectively. The larger data points (●) with bar (at 165 and 330 mM KCl) represent the mean of 24 and 6 individually performed experiments, respectively. All data points (n = 113) were fitted by nonlinear regression analysis to simple Michaelis-Menten kinetics including a modifier term (Eq. T8). The best fit was obtained with a value for J^a_{max} of 445 (SD 20) pmol cm^{-2} s, a value for K^a_{Cl} of 29.5 (SD 3.1) mM, and a value for K_m of 452 (SD 73) mM.

determined from the intersection with the heavily dashed line, which represents the mean reference value of $1/J$ obtained at $[Cl_o]$ = 165 mM in all experiments. The pK_4 value corresponding to the mean intersection value was found to be 9.36 (SD 0.07).

The slopes of the lines in Fig. 5 *C*, together with the slope at 16.5 mM $[Cl_o]$ obtained from the data in Fig. 12 *B* (with $[Cl_i]$ = 165 mM and pH_o in the interval 8–9.6), were further plotted as a function of $1/[Cl_o]$ (Fig. 5 *D*). This should give a straight line passing through the origin and having a slope equal to $K_4 \cdot K^a_{Cl}/ [(A^a + 1) \cdot J^a_{max}]$ as can be deduced from Eq. T9. The slope (2.17 [SD 0.26] 10^{-3} M^2 cm^2 s mol^{-1})

and the intercept (2.1 [SD 5.7] 10^{-2} M cm^2 s mol^{-1}) of the dashed line were obtained from a nonlinear plot of the slopes vs. $[Cl_o]$ (with statistical weighting of the data). A slight deviation from the origin prediction is to be expected because the relation (Eq. T9) is only approximate. The result indicates that the data within experimental error do not contradict the model assumptions.

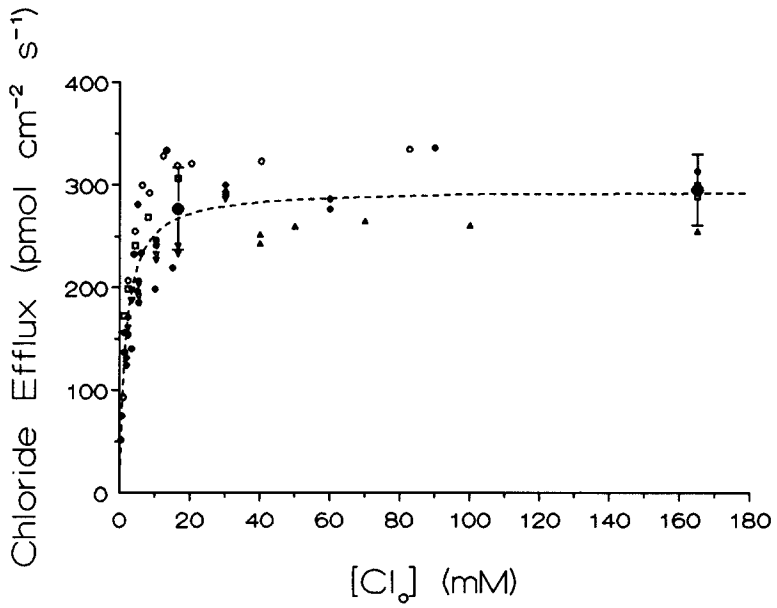

FIGURE 4. Chloride self-exchange flux as a function of $[Cl_o]$ at pH_o 8.0, $[Cl_i]$ = 165 mM, and 0°C, used for determination of the asymmetry factor A^a. ● represents single determinations made on different days. The larger data points (●) with bar (at 16.5 and 165 mM KCl) represent the mean of 12 and 20 individual experiments, respectively, with the bars representing the SD. The other data points (○, □, ▽, △) represent series of results obtained with the same preparation of resealed ghosts. The curve shows the best nonlinear fit to all points (n = 98) assuming simple Michaelis-Menten kinetics. The best fit was obtained with a value for K_o^{app} of 1.64 (SD 0.18) mM and an apparent value for J_{max}^{app} of 299 (SD 5) pmol cm^{-2} s. The values of the asymmetry factor A^a and J_{max}^a were similarly determined by direct nonlinear fitting to Eq. T7 using the values for K_{Cl}^a and K_m^{Cl} determined from Fig. 3. The value of A^a was found to be 10.7 (SD 1.3) and that of J_{max}^a 457 (SD 8) pmol cm^{-2} s^{-1}.

Determination of the pK of the Second Deprotonatable Group

The pK of the second deprotonatable group, pK_5, was determined at alkaline pH_o (11–12.5) using Eq. 10, with conditions where the first group should be nearly completely deprotonated. The chloride self-exchange was measured at three different $[Cl_o]$'s (30, 90, and 165 mM) as a function of pH_o with the same preparation of ghosts. Plots of the data in the form of $1/J$ vs. $1/[H_o]$ at each $[Cl_o]$, shown in Fig. 6 *A*, appears to give straight lines, passing through the same point (defining pK_5), as demonstrated when fitted to simple linear regression. An intrinsic pK_5 value of 11.34

(SD 0.08) was obtained from the abscissa value of the intersection point (equal to $-1/K_5$).

A plot of the slopes of the lines (from Fig. 6 *A*) as a function of $1/[Cl_o]$ is shown in Fig. 6 *B*. According to the model the points should be located on a straight line (with a slope corresponding to $K_5 \cdot K_{Cl}^b / [(A^b + 1) \cdot J_{max}^b]$ passing through the origin, indicat-

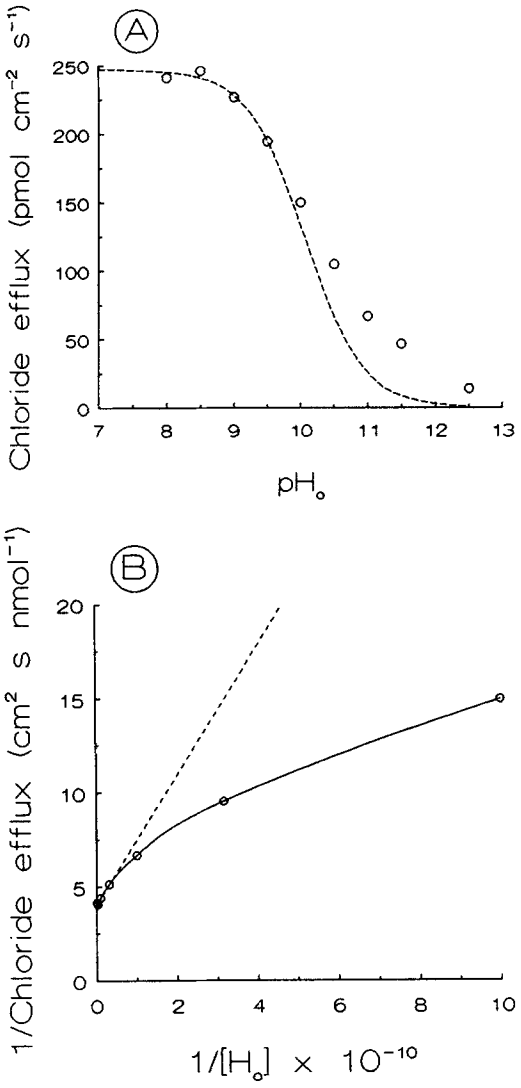

FIGURE 5. (*A*) Chloride self-exchange vs. pH_o at $[Cl_o]$ = 10 mM. Initial $[Cl_i]$ = 165 mM, pH 7.3, 0°C. The apparently sigmoid experimental curve does not follow a simple titration function (*dashed curve*). (*B*) The data of *A* plotted as $1/J$ vs. $1/[H_o]$ reveals that a simple pH dependency is only seen for the initial part of the curve (*dashed line*). The curvature of the plot at higher pH values (above pH 9.7 as determined from this experiment) is to be expected from the model (Eq. T6). The approximately linear initial part of the curve was used to determine the intrinsic titration constant K_4, as demonstrated in *C*.

ing that negligible chloride is bound to the titratable group when this group is deprotonated. The slope of the line in Fig. 6 *B* was found to be 3.44 (SD 0.27) 10^{-4} M^2 cm^2 s mol^{-1} and the intercept 7.1 (SD 5.5) 10^{-4} M cm^2 s mol^{-1}. The positive low intercept value indicates that the S_oCl_o form may exist but only in so low a

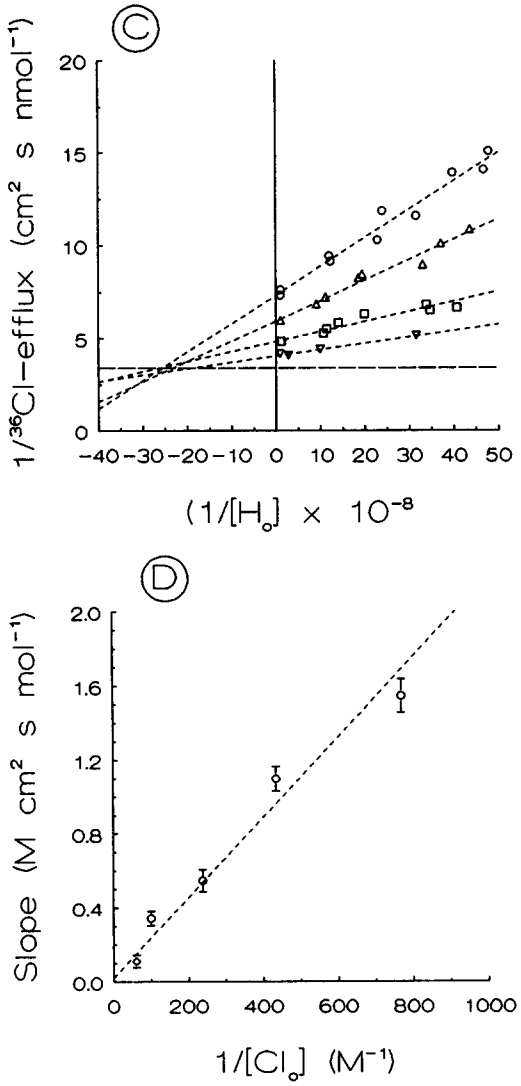

FIGURE 5 *(continued).* (*C*) Determination of the intrinsic constant K_4. The initial straight part of the curve (Fig. 5 *B*) was examined in relation to similar curves at lower $[Cl_o]$ in the pH interval from 8 to 9.7. Since the individual set of data points at $[Cl_o]$ = 1.3 mM (○), 2.3 mM (△), 4.2 mM (□), and 10 mM (▽) were obtained on different days, the different sets of transport data were normalized to the transport value at 165 mM KCl, pH 8.0, obtained in each experiment in order to eliminate the inter-day variation. All data points are thus presented relative to the mean chloride self-exchange of 295 pmol cm^{-2} s^{-1} at 165 mM $[Cl_o]$, pH 8, in the four experiments. This value is represented by the horizontal dashed line. The chloride self-exchange at each $[Cl_o]$ as a function of pH_o was fitted nonlinearly to a simple titration function (not shown) before transformation of the data into the plot of $1/J$ vs. $1/[H_o]$ using the parameters, apparent pK_o and apparent J_{max}, obtained. The straight lines obtained by this transformation intersect close to the same point to the left of the ordinate. The abscissa of this intersection point represents $-1/K_4$ according to the model (cf. Eq. T9) and corresponds to an intrinsic constant K_4 of $10^{-9.36}$ (SD 0.07 pK unit) as determined from the intersections with the horizontal line. (*D*) The slopes of the lines in *C*, and the slope at 16.5 mM $[Cl_o]$ (◇) (obtained from the data of Fig. 12 *B*) plotted as a function of $1/[Cl_o]$. The bar represents the SD of the slope obtained by the nonlinear fitting of the individual curves.

concentration that it does not contradict the model predictions within experimental error.

Determination of the Ratio D between J^b_{max} and J^a_{max}

An approximate value of the parameter D can be obtained at high $[Cl_i]$ as the ratio between the apparent J_{max} values at alkaline pH_o and neutral pH (see Eq. T11). Plots

of $1/J$ vs. $1/[Cl_o]$ (at high $[Cl_i]$ = 330 mM) at alkaline pH_o (pH 12) and neutral pH_o (pH 8) are shown in Fig. 7. The figure shows the mean of three sets of experiments, with the bars indicating SD. An apparent maximal efflux at $J_{max}^{app\ pH_o12}$ = 418 (SD 53) pmol cm^{-2} s^{-1}, a $K_o^{app\ pH_o12}$ = 353 (SD 71) mM, and a $J_{max}^{app\ pH_o8}$ = 257 (SD 4) pmol cm^{-2} s^{-1} were obtained by nonlinear fit of the data to simple Michaelis-Menten

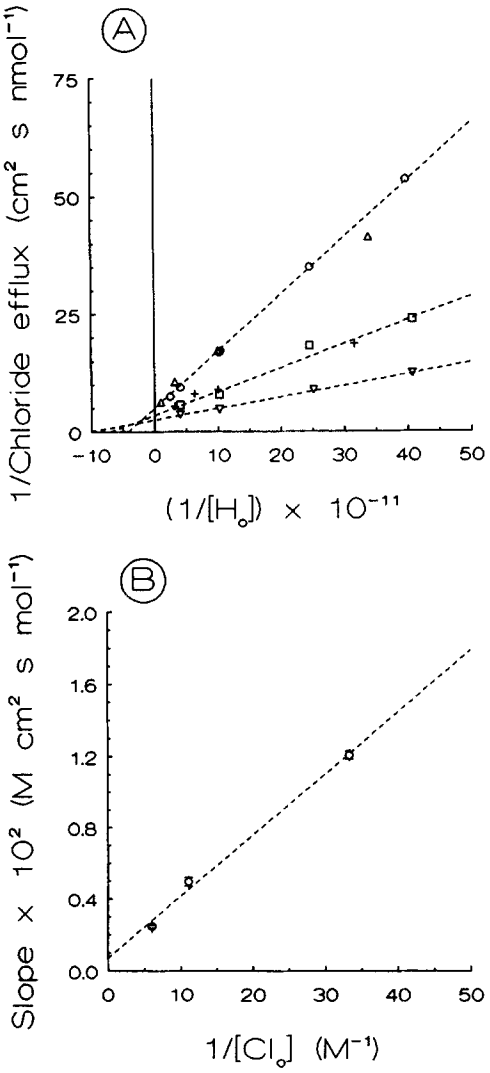

FIGURE 6. Determination of the intrinsic constant K_5. The chloride self-exchange was measured at three $[Cl_o]$, 30 mM (○), 90 mM (□), and 165 mM (▽), as a function of pH in the pH interval (11.6–12.8). The three sets of data points were obtained for the same preparation of resealed ghosts. The other data points (△, +) were obtained on different days and normalized through their transport at $[Cl_o]$ = 165 mM, pH 8 to the first set of data. The data were plotted as described in Fig. 5 *C*. The three lines obtained in the plot showing $1/J$ vs. $1/[H_o]$ intersect close to the same point to the left of the ordinate with an abscissa value that corresponds to $K_5 = 10^{-11.34}$ (SD 0.08 pK unit). (*B*) The slope of the lines in *A*, plotted as a function of $[Cl_o]$. The positive intercept value with the ordinate 7.1 (SD 5.5) 10^{-4} M cm^2 s mol^{-1} indicates that the S_oCl_o form may exist but in so low a concentration that the proposed model within experimental error is capable of explaining the obtained data.

kinetics. The data at pH 8 were fitted to only one variable, using the value for $K_o^{app\ pH_o8}$ obtained from Fig. 4. The ratio of the two apparent J_{max} values ($J_{max}^{app\ pH_o12}/J_{max}^{app\ pH_o8}$) which corresponds to the intercepts of the two straight lines with the ordinate, gave an approximate value for D of 1.63 (SD 0.21). The true value is likely to be ~1.5% lower as estimated from Eq. T11 and model constants in Table III.

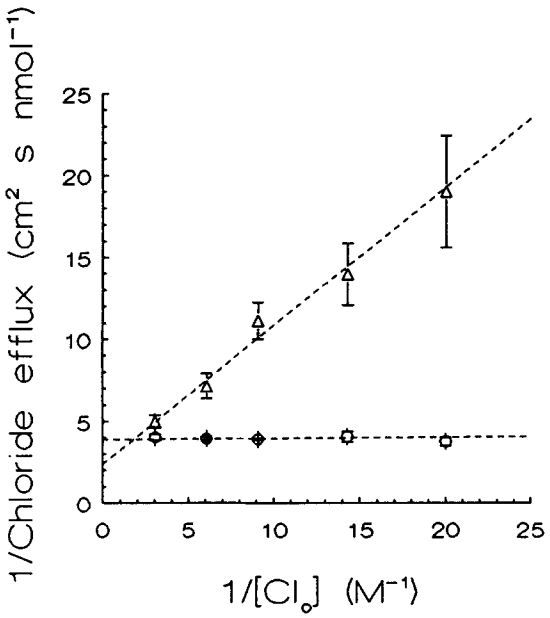

FIGURE 7. The apparent maximal efflux rate at pH_o 8.0 and pH_o 12.0, shown in the form of a Lineweaver-Burk plot at $[Cl_i]$ = 330 mM, pH_i 7.3, used for determination of the ratio, D, between J_{max} in the neutral (□) and alkaline (△) state. The J_{max}^{app} and K_o^{app} values at pH_o 12 were obtained from the data, J vs. $[Cl_o]$, by nonlinear fit to simple Michaelis-Menten kinetics. The value of J_{max}^{app} at pH_o 8.0 was obtained by nonlinear fit to simple Michaelis-Menten kinetics using a value for K_o^{app} of 1.7 mM, determined from Fig. 4. The dashed lines show the best fit in a reciprocal replot based on three sets of experiments performed on different days, with the bars indicating the SD on the different data points. The ratio between J_{max}^{app} at pH_o 12 and pH_o 8 gave a value for D of 1.63 (SD 0.21).

Determination of the Ping-Pong Parameters in the Alkaline State

The value for the asymmetry factor A^b at alkaline pH_o, chloride self-exchange experiments was obtained at pH 11.6 (0°C) with $[Cl_i]$ and $[Cl_o]$ varying between 16.5 and 66 mM. It was estimated (from model calculations) that >95% of the transport under these conditions is mediated by the alkaline system. The chloride self-

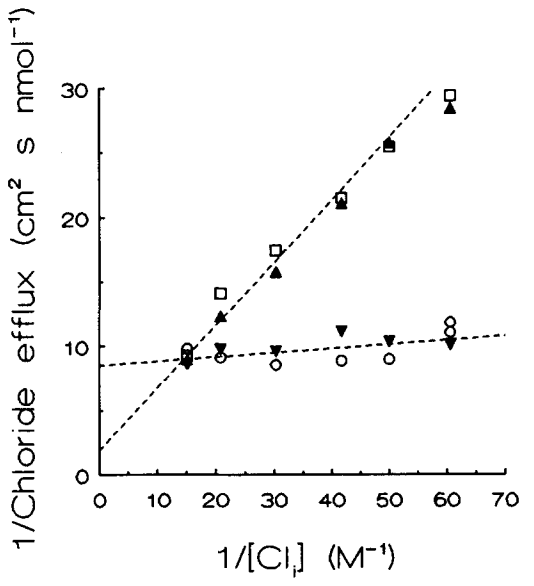

FIGURE 8. Determination of the asymmetry factor A_b at alkaline pH_o 11.6, 0°C. Resealed citrate ghosts initially containing 16.5 mM KCl were prepared as described in Materials and Methods. The two dashed lines represent the best linear fit to the data with $[Cl_i] = [Cl_o]$ (□, ▲) and to the data with constant $[Cl_o]$ (66 mM) and varying $[Cl_i]$ (○, ▼), respectively, pH_i 7.3 and pH_o 11.6 at 0°C. The results (□, ○) and (▲, ▼) were obtained on two different days. The value for A^b was determined from the ratio between the slopes of the lines to be 0.21 (SD 0.07) (cf. Eq. T13b).

exchange vs. $[Cl_i]$ with $[Cl_o] = [Cl_i]$ and $[Cl_o]$ kept constant at 66 mM and varying $[Cl_i]$ is shown in Fig. 8. The data were nonlinearly fitted to Eqs. T12a and T13a and the data points and theoretical curves transformed into Lineweaver-Burk plots. The asymmetry factor, A_b, was determined from the ratio between the slope of the line with $[Cl_o] = [Cl_i]$ (S_1 = 47.3 [SD 2.72] 10^{-2}) and with $[Cl_o]$ = 66 mM (S_2 = 3.27 [SD 1.04] 10^{-2}), determined by direct nonlinear fit to the data. The ratio between the slopes equal to $[1 + (K_5/[H_o]) + A_b]/A_b$ (Eq. T13b) was found to be 14.5 (SD 4.6). Using the value for pK_5 of 11.35, the value for A_b was found to be 0.21 (SD 0.07).

The K^b_{Cl} constant was determined from Eq. T10 by direct nonlinear fit of J vs. $[Cl_o]$ at different alkaline pH_o values. The previously obtained constants $K_5 = 10^{-11.35}$ and $A^b = 0.2$ were inserted. The results from seven such experiments are shown in Table II. The found mean value for the free parameters J^b_{max} and K^b_{Cl} were 726 (SD 72) pmol cm^{-2} s and 110 (SD 14) mM, respectively.

TABLE II

Determination of K^b_{Cl}

Experiment	pH_o	Chloride	K^b_{Cl} (SD)	J^b_{max} (SD)
		mM	*mM*	*pmol cm^{-2} s^{-1}*
1	11.6	Cl_i = 165	115 (20)	765 (80)
2	11.6	Cl_i = 165	95 (7)	761 (32)
3	12.0	Cl_i = 165	97 (19)	730 (102)
4	12.0	Cl_i = 165	114 (50)	810 (262)
5	12.1	Cl_i = 165	102 (12)	691 (66)
6	12.0	Cl_i = 330	135 (25)	740 (86)
7	11.6	$Cl_i = Cl_o$	113 (34)	584 (145)
Mean (SEM)			110 (14)	726 (72)

Chloride self-exchange as a function of $[Cl_o]$ and $[Cl_i]$ was fitted by nonlinear regression to the equations for chloride self-exchange at alkaline pH_o (Eq. T10). The alkaline asymmetry factor $A^b = 0.2$ (Fig. 8) and $pK_5 = 11.35$ (Fig. 6) were used and the data were fitted with the free variables K^b_{Cl} and J^b_{max}. Experiments 1–5 were performed with resealed ghosts with $[Cl_i]$ = 165 mM and 30 mM < $[Cl_o]$ <165 mM. Buffers: 0.5 mM phosphate, 0.5 mM CHES. The results of experiments 6 and 7 were replots of the alkaline data from Figs. 7 and 8 (with $[Cl_i] = [Cl_o]$), respectively.

TESTING THE PROPOSED MODEL

To test the proposed model, chloride self-exchange was examined as a function of pH_o for various values of $[Cl_i]$ and $[Cl_o]$. The experimental data were compared with the theoretical curves obtained by the model using Eq. T6 and the model constants from Table III.

Extracellular Titration with Constant $[Cl_i]$ = 165 mM KCl

The chloride self-exchange as a function of pH_o at various $[Cl_o]$ and constant $[Cl_i]$ of 165 mM KCl is shown in Fig. 9. The data were normalized to the chloride self-exchange obtained at pH_o 8.0. The theoretically determined dashed curves

TABLE III

The Observed Transport Constants

Experiment	Constant	Determined value (SD)	Value used in model
Fig. 3	K^a_{Cl}	29.5 (3.1) mM	30 mM
	K_m	452 (73) mM	450 mM
	J^a_{max}	445 (20) pmol cm^{-2} s^{-1}	
Fig. 4	A^a	10.7 (1.3)	10.7
Fig. 5	pK_4	9.36 (0.08)	9.4
Fig. 6	pK_5	11.34 (0.08)	11.35
Fig. 7	D	1.63 (0.21)	1.7
Fig. 8	A^b	0.206 (0.071)	0.2
Table II	K^b_{Cl}	110 (14) mM	110 mM
	J^b_{max}	726 (72) pmol cm^{-2} s^{-1}	
	Constants Related to Iodide Binding		
Fig. 14	K^I_m	121 (62) mM	
	K^I_o	1.06 (0.15) mM	
	$K^{I'}_o$	38 (14) mM	
	pK_6	10.9	

closely fit the experimental data at all [Cl_o] tested (1.8–165 mM). This is also the case for the data shown by the small inverted triangles at 165 mM [Cl_o], which are from Fig. 1 of Wieth and Bjerrum (1982). The apparent pK values, simply defined as the pH_o values giving half-maximal chloride efflux, at 2, 8, 16, 30, 90, and 165 mM KCl_o are ~9.8, 10.35, 10.75, 11.2, 11.8, and 12, respectively.

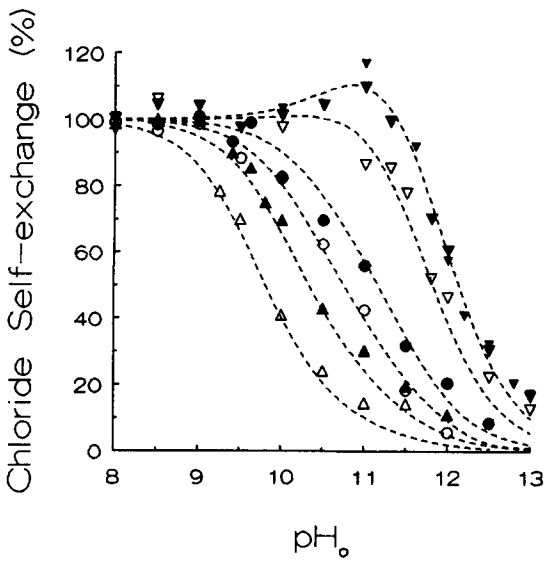

FIGURE 9. Extracellular titration of the anion transport system at 0°C and constant [Cl_i] = 165 mM. [Cl_o]: 1.8 (△), 8 (▲), 16.5 (○), 30 (●), 90 (▽), and 165 mM (▼). The small filled triangles are the 165 mM KCl data from Fig. 1 of Wieth and Bjerrum (1982). The magnitude of the fluxes were calculated relative to the flux at each [Cl_o] at pH 8.0. These reference fluxes were 155, 254, 262, 258, 336, and 276 pmol cm^{-2} s^{-1}, respectively. The dashed curves were calculated from Eq. T6 using the values for the different constants presented in Table III. The apparent pK values are ~9.8, 10.35, 10.75, 11.2, 11.8, and 12, respectively.

Testing the Model under Conditions with [Cl$_i$] = [Cl$_o$]

The model was further tested under conditions of [Cl$_i$] = [Cl$_o$]. The results obtained (shown in Fig. 10) were normalized according to the chloride self-exchange at pH$_o$ 8 in the different sets of experiments. The dashed curves represent the theoretical titration curves calculated from Eq. T6 using the determined constants given in Table III. It can be calculated that the apparent pK$_o$ (determined at half-maximal efflux) approaches a limit of ~10.8 when the chloride concentrations reduced toward zero under conditions of [Cl$_o$] = [Cl$_i$]. With higher [Cl] the model fits the alkaline stimulation "hump." This is also the situation with the small circles in Fig. 10, which are the 330 mM data from Fig. 4 of Wieth and Bjerrum (1982).

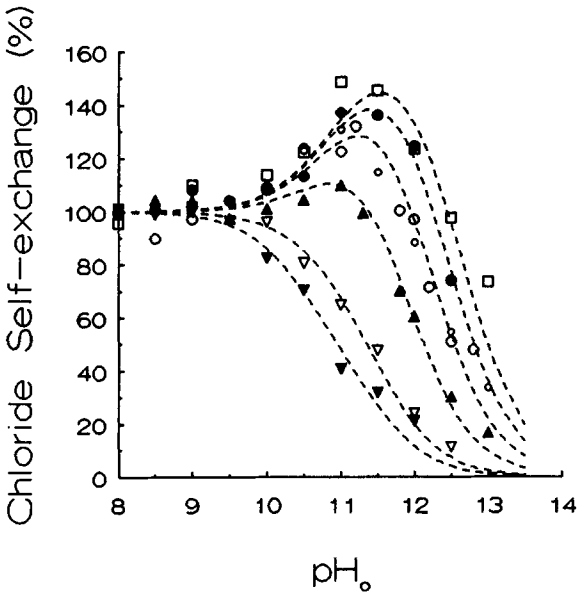

FIGURE 10. Extracellular titration of chloride self-exchange at 0°C with [Cl$_i$] = [Cl$_o$]: 4.5 (▼), 30 (△), 165 (▲), 330 (○), 500 (●), and 660 mM KCl (□). The small circles are the 330 mM KCl data from Fig. 4 of Wieth and Bjerrum (1982). Extracellular buffer: 0.5 mM CHES and 2 mM phosphate, except at 4.5 mM, where only 0.5 mM CHES and 0.5 mM phosphate buffer were used. At [Cl$_i$] below 165 mM, the ionic strength (both intra- and extracellular) was kept constant by citrate substitution. The symmetrical [Cl] at higher concentrations was obtained by shrinkage of the ordinary resealed ghosts. The magnitude of the chloride fluxes was calculated relative to the values found at pH 8.0. These reference fluxes were: 44 (▼), 260 (▽), 277 (▲), 249 (○), 240 (●), and 192 pmol cm^{-2} s^{-1} (□). The dashed curves represent the theoretical efflux values calculated from Eq. T6 using the constants in Table III.

Effects of Transport Coupled Conformational Changes

The proposed model predicts that the apparent pK$_o$ should be sensitive to variations in the chloride gradient across the membrane under conditions of constant [Cl$_o$]. To test this, experiments were performed under conditions where this effect should be pronounced. Fig. 11 shows the effect on the titration curve when [Cl$_i$] is increased by a factor of 36 with [Cl$_o$] = 1.8 mM (Fig. 11 *A*) and [Cl$_o$] = 6 mM (Fig. 11 *B*), respectively. The changes in apparent pK were 0.5 and 0.9 pH units, respectively. Both changes are in accordance with theoretical expectations (dashed curves) obtained using only the determined constants compiled in Table III. At high [Cl$_o$], a change in the anion transport stimulation at alkaline pH, "the modifier hump,"

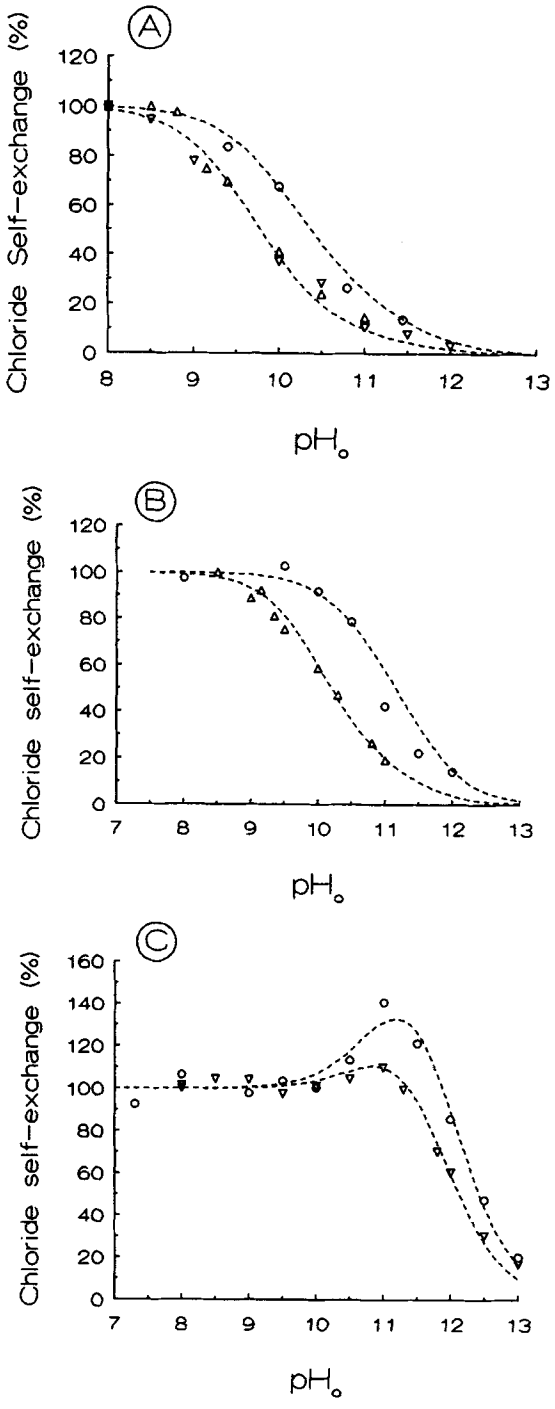

FIGURE 11. Chloride self-exchange as a function of pH_o at three different $[Cl_o]$'s. The effect of changing $[Cl_i]$ on the transport function (recruitment) is demonstrated at 0°C. (*A*) Outward recruitment (▽, △). Experiments were performed on resealed ghosts containing 165 mM KCl. Efflux medium: isotonic 1.8 mM KCl, sucrose citrate substituted. Inward recruitment (○). Resealed potassium citrate–containing ghosts with 4.5 mM $[Cl_i]$. Efflux medium: 1.8 mM KCl, 25 mM potassium citrate. (*B*) Outward recruitment (△). Experiments were performed on resealed ghosts containing 165 mM KCl. Efflux medium: 6 mM KCl, substituted with isotonic sucrose citrate medium. Inward recruitment (○). Reseale potassium citrate–containing ghosts with 4.5 mM $[Cl_i]$. Efflux medium: 6 mM KCl, 25 mM potassium citrate. (*C*) Outward recruitment (▽). Experiments were performed on resealed ghosts containing 165 mM KCl. Efflux medium 165 mM KCl. Inward recruitment (○). Resealed sucrose-containing ghosts with 16.5 mM $[Cl_i]$. Efflux medium: 165 mM KCl. The magnitudes of the chloride fluxes were calculated relative to the values found at pH 8.0. These reference fluxes were: (*A*) 155 (▽), 132 (△), and 57 pmol cm^{-2} s^{-1} (○); (*B*) 276 (○) and 41 pmol cm^{-2} s^{-1} (△); and (*C*) 276 (▽) and 143 pmol cm^{-2} s^{-1} (○). The dashed curves were calculated using Eq. T6 and the constants in Table III.

should also be expected when $[Cl_i]$ is changed. This effect was tested (Fig. 11 *C*) by reducing $[Cl_i]$ to 16.5 mM, while keeping $[Cl_o]$ at 165 mM. This change in $[Cl_i]$ modulates the transport stimulation significantly, as predicted from the model constants (Table III; used to calculate the dashed curves). These results therefore provide further support that the modifier hump is related to titration of the two titratable groups and that the data are consistent with a ping-pong mechanism at alkaline pH. The recruitment effect was also observed at 8 and 16 mM $[Cl_o]$, when $[Cl_i]$ was reduced from 165 mM to 8 and 16 mM, respectively (Fig. 12, *A* and *B*), but the effect was reduced owing to the less pronounced change in the chloride gradient. The effect had nearly vanished (0.15 pK units) when $[Cl_o]$ was 30 mM and $[Cl_i]$ was reduced from 165 to 30 mM (Fig. 12 *C*).

K_o Apparent and J_{max} Apparent as a Function of pH_o

The values for J_{max}^{app} and K_o^{app} obtained at various pH_o and a constant $[Cl_i]$ are shown in Fig. 13, *A* and *B*. K_o^{app} apparently increases exponentially as a function of increasing pH (Fig. 13 *A*). This increase is in accordance with the theoretical curve calculated from the constants in Table III. It can be seen from Fig. 13 *B* that J_{max}^{app} has a constant value at neutral pH, but gradually increases and reaches a new stable value at alkaline pH. The change takes place with an apparent pK of ~11. The observed change is in accordance with the theoretical curve (i.e., the dashed curve calculated from Eq. T6), using the observed constants in Table III. Unfortunately, the K_o^{app} and J_{max}^{app} values could not be determined properly from a Michaelis-Menten plot at $pH_o > 12$ because the values are too interdependent when the maximal $[Cl_o]$ (which it is possible to use with $[Cl_i]$ = 165 mM) is significantly lower than K_o^{app}; however, the ratio K_o^{app}/J_{max}^{app} can be determined at this high pH value. Fig. 13 *C* shows that K_o^{app}/J_{max}^{app} appears to increase linearly with increasing alkaline pH_o, as also predicted from the model.

Effects of Extracellular Iodide Inhibition

In the paper by Wieth and Bjerrum (1982) it was observed that iodide influences the modifier hump strongly. To see whether the present model could simulate this effect and to get an idea of the size of the involved competitive iodide binding constants in the neutral and alkaline state, the model was expanded to include I_o binding (see Fig. 1). Iodide is transported ~260 times more slowly than chloride (Dalmark and Wieth, 1972) and may thus act as a simple extracellular inhibitor with the short efflux times used in the ^{36}Cl efflux measurements. Iodide inhibits chloride self-exchange from the exofacial side by two different mechanisms, namely, competitively by binding to the anion transport site and by binding to an extracellular modifier site (as demonstrated in Fig. 14 *A*). To treat the complex inhibition observed, several simplifying assumptions were made as explained in the Theory section. The constant for I_o modifier inhibition K_m^I (the extracellular iodide self-inhibition constant) was determined from the data of Fig. 14 *A*. The figure shows the chloride self-exchange expressed as the reciprocal of the fraction of transport at $[I_o]$ = 0 plotted as a function of $[I_o]$ under conditions where $[Cl_i]$ = 165 mM and $[Cl_o]$ = 16.5 mM (pH 8.0 and 0°C). The data were nonlinearly fitted to Eq. T15 with the free parameters $K_o^{I\,app}$ (the apparent

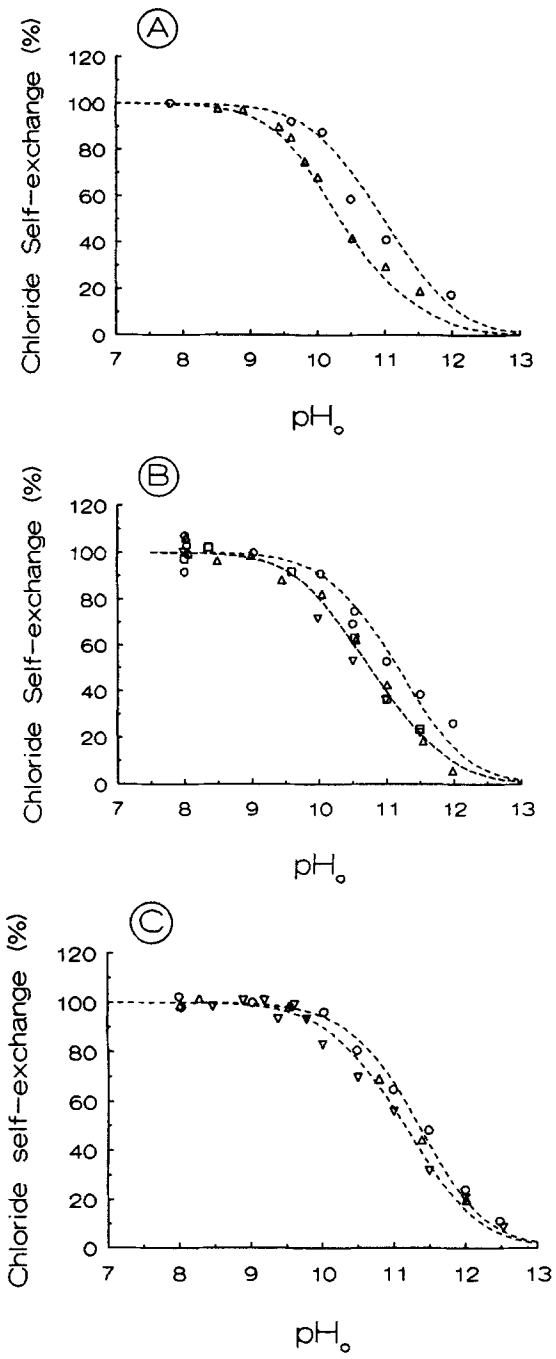

FIGURE 12. Chloride self-exchange as a function of pH_o, $[Cl_o]$ = 8, 16, and 30 mM. Comparison between conditions where $[Cl_i]$ = $[Cl_o]$ and $[Cl_i]$ = 165 mM. (*A*) ^{36}Cl efflux from citrate-containing resealed ghosts (8 mM KCl, 25 mM potassium citrate) vs. pH_o in 8 mM KCl, 25 mM potassium citrate (○) compared with efflux from ordinary resealed ghosts with $[Cl_i]$ = 165 mM in a medium with $[Cl_o]$ = 8 mM and substituted with sucrose citrate (△). (*B*) As described for *A* but with $[Cl_o]$ = 16.5 mM. Symmetrical [Cl] (○), asymmetrical [Cl] (▽, △, □). (*C*) As described for *A* but with $[Cl_o]$ = 30 mM. Symmetrical [Cl] (○), asymmetrical [Cl] (▽, △). The magnitudes of the chloride fluxes are shown relative to the values found at pH 8.0. These reference fluxes are: (*A*) 120 (○) and 261 pmol cm^{-2} s^{-1} (△); (*B*) 145 (○), 331 (▽), 247 (△), and 308 pmol cm^{-2} s^{-1} (□); (*C*) 260 (○), 258 (▽), and 280 pmol cm^{-2} s^{-1} (△). The dashed curves were calculated from Eq. T6 and the constants in Table III, and demonstrate that the experimental data are in accordance with the model within experimental error.

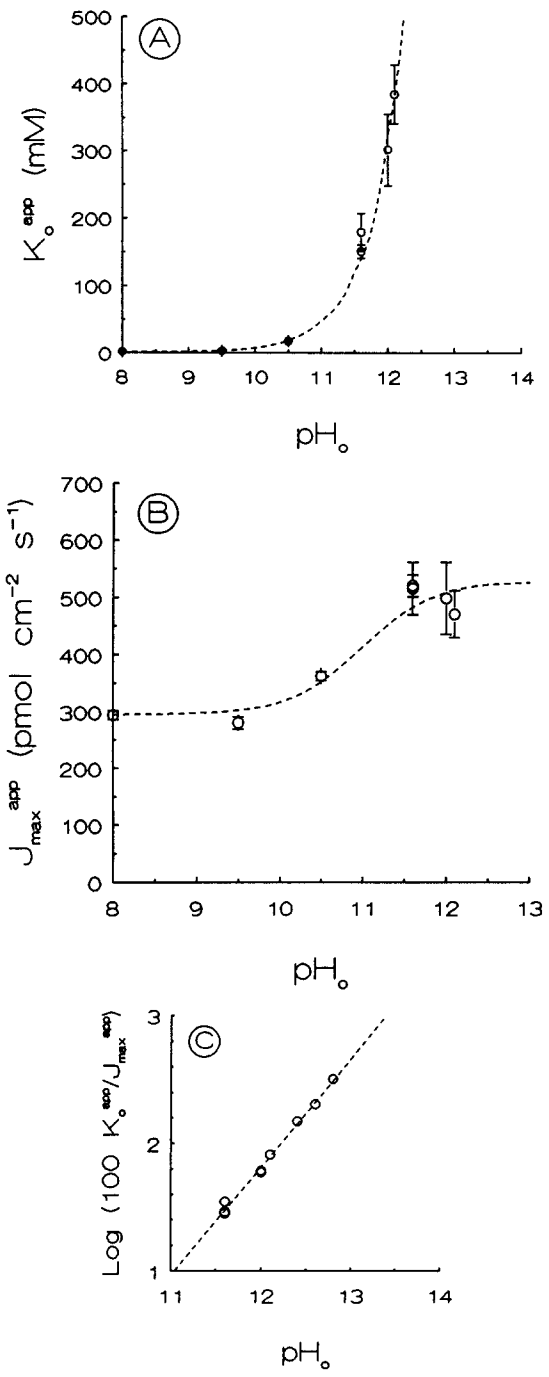

FIGURE 13. (*A*) The apparent extracellular half-saturation constant for chloride binding K_o^{app} as a function of pH_o. The parameters K_o^{app} and J_{max}^{app} were obtained by nonlinear fit to the simple Michaelis-Menten equation for chloride self-exchange data as a function of $[Cl_o]$, obtained at various alkaline pH_o values. Ghosts: initially 165 mM KCl, 2 mM Tris. Medium: Isotonic chloride media substituted with sucrose citrate. The bars indicate the SD obtained in the nonlinear fit to the individual set of data. The dashed lines show the theoretical values of K_o^{app} obtained from the constants in Table III. (*B*) The apparent J_{max}^{app} for chloride transport at various pH_o values obtained as explained for *A*. The dashed line shows the theoretical values for J_{max}^{app} as a function of pH, obtained from the constants in Table III and the value for J_{max}^{app} at pH 8 of 299 pmol cm^{-2} s, obtained from Fig. 4. The K_o^{app} (*A*) and J_{max}^{app} (*B*) could not be determined with accuracy at pH values above 12.1, but the ratio K_o^{app}/J_{max}^{app} is a well-defined parameter even at higher pH values, as demonstrated in *C*. (*C*) Plot of log (100 K_o^{app}/J_{max}^{app}) as a function of pH_o. The data are from *A* and *B* and from Fig. 6 at pH > 12. The data were replotted as chloride self-exchange vs. $[Cl_o]$ at various pH_o values, and the ratio $R = K_o^{app}/J_{max}^{app}$ was determined by nonlinear fits to the equation $J = [Cl_o]/[R + ([Cl_o]/J_{max}^{app})]$. Only R is reasonably well-defined in these plots (as explained in Results).

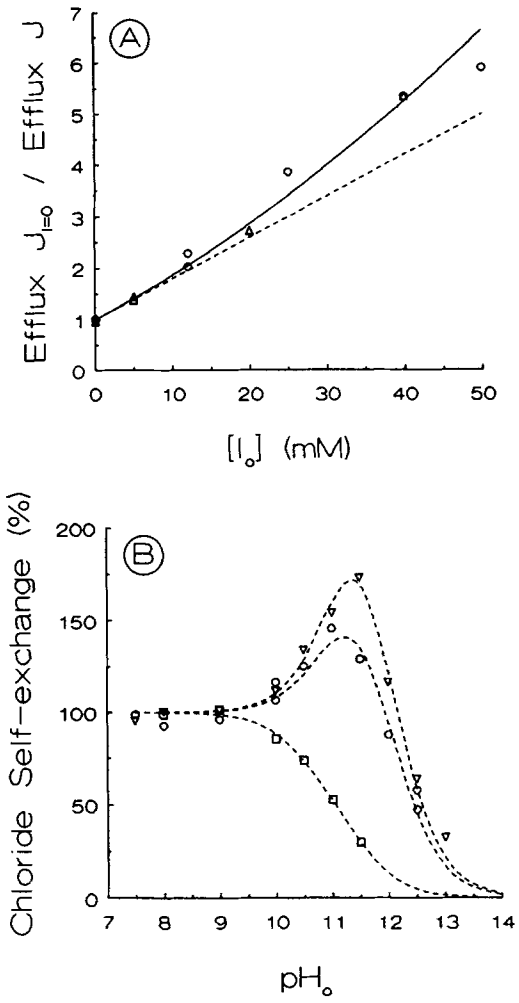

FIGURE 14. (*A*) Determination of the binding constant for extracellular noncompetitive iodide inhibition, K_m^I. The figure shows $J_{I=0}/J$ as a function of $[I_o]$. Ghosts: initial $[Cl_i]$ = 165 mM, 2 mM Tris. Medium: 16.5 mM $[Cl_o]$, *X* mM I_o, 0.5 mM phosphate, substitution of Cl_o and I_o with 25 mM citrate, 200 mM sucrose medium to isotonicity. The experimental data (○, △) obtained at two different days were fitted directly to the equation for competitive and noncompetitive inhibition (Eq. T15) with the free parameters $K_o^{I\,app}$ and K_m^I, and transformed to the Dixon plot shown. The best fit was obtained with an apparent competitive iodide inhibition constant $K_o^{I\,app}$ of 12.5 (SD 1.0) mM and a noncompetitive inhibition constant K_m^I of 121 (SD 62) mM. The value of K_m^I was used in connection with *B*. (*B*) Chloride self-exchange as a function of pH_o at 0°C in the presence of three different extracellular $[I_o]$'s and $[Cl_o]$'s. Ghosts: initial intracellular pH 7.3, 165 mM KCl, 2 mM Tris. Media: (▽) 105 mM KI, 60 mM KCl; buffer: 2 mM phosphate, 0.5 mM CHES; (○) 60 mM KI, 105 mM KCl (data from Wieth and Bjerrum, 1982, Fig. 5); and (□) 10 mM KI, 10 mM KCl, 1 mM TES, CHES, and CAPS, respectively. The experimental data were fitted to the iodide inhibition model (Eq. T14), with the free variables J_{max}, K_o^I, and $K_o^{I'}$. This last value was free only in the experiments with 105 and 60 mM iodide. A value of 38 mM for $K_o^{I'}$ was used in the experiment with 10 mM I_o. The iodide self-inhibitor constant K_m^I was obtained from *A* and the other constants from Table III. The following values were obtained: (▽) J_{max} = 569 (SD 55) pmol cm^{-2} s^{-1}, K_o^I = 1.05 (SD 0.13) mM, and $K_o^{I'}$ = 41 (SD 10) mM; (○) J_{max} = 421 (SD 59) pmol cm^{-2} s^{-1}, K_o^I = 0.95 (SD 0.24) mM, and $K_o^{I'}$ = 35 (SD 17) mM; (□) J_{max} = 599 (SD 18) pmol cm^{-2} s^{-1}, and K_o^I = 1.19 (SD 0.08) mM. The figure shows the results after normalization with the reference efflux values obtained at neutral pH. These reference efflux values are 56, 94, and 143 pmol cm^{-2} s^{-1}, respectively.

competitive inhibitor constant) and K_m^I. By this procedure values of $K_o^{I\,app} = 12.5$ (SD 1.0) mM and $K_m^I = 121$ (SD 62) mM were determined.

K_o^I and $K_o^{I'}$ were determined from plots of ^{36}Cl efflux vs. pH_o (Fig. 14 *B*) by a simple nonlinear fit to Eq. T14, using the constants already determined in Table III, including the I_o self-inhibition constant K_m^I determined from Fig. 14 *A* and assuming that $K_m^I = K_m^{I*}$ as justified below. K_m^{I*} is the I_o modifier binding constant when the substrate site is loaded with chloride. Three sets of data were obtained with the free parameters J_{max}^a, K_o^I, and $K_o^{I'}$ and with $[Cl_i] = 165$ mM and different values of $[I_o]$ and $[Cl_o]$. The constant $K_o^{I'}$ was only a free variable in the experiments with 60 and 105 mM I_o. The mean values obtained in these two experiments were used as constants in the experiment with 10 mM I_o. The data with 60 mM I_o are from Fig. 5 of Wieth and Bjerrum (1982). The dashed curves show the best fit obtained when the individual sets of data were fitted to Eq. T14. The mean values of K_o^I and $K_o^{I'}$ of the individual determinations were found to be 1.06 (SD 0.15) mM and 38 (SD 14) mM, respectively (see legend to Fig. 14 for the values obtained in the different sets of experiments). The assumption that $K_m^I = K_m^{I*}$ was used because the K_m^{I*} value is difficult to obtain precisely and because this parameter has no effect on the determined J_{max}^a and $K_o^{I'}$ and only a small effect on the K_o^I value. The mean value of K_o^I from the three experiments only changed from 0.96 to 1.4 mM when the K_m^{I*} value was varried from ∞ to 40 mM. The calculated effect is probably even overestimated because the model (for the sake of simplicity) also includes I_o binding to the inward-facing, chloride-loaded form.

The quantitative effect of an alkaline modifier effect is also considered. If a noncompetitive extracellular modifier constant $K_m^{I'}$ of 121 mM is included at alkaline pH_o, the $K_o^{I'}$ increases to ~90 mM, with K_o^I and J_{max}^a nearly unchanged. Since the alkaline modifier inhibition effect, if it exists, is likely to be less than that at neutral pH, it is safe to conclude that K_o^I is likely to be 1–1.5 mM, a value not very different from the value obtained by Milanick and Gunn (1986) and with $K_o^{I'}$ a factor of 25–50-fold higher.

DISCUSSION

The results presented here show that the anion transport process at alkaline pH_o and neutral pH_i can be described by a kinetic model involving two types of functionally important positive deprotonatable groups located on the exofacial side of the membrane (Fig. 1). The group with the higher pK, moreover, appears to be functionally essential. The model both qualitatively and quantitatively describes the chloride transport process at $pH_o > 8$, including the stimulation of chloride self-exchange with the reversible competitive I_o inhibition at alkaline pH. The magnitude of chloride self-exchange as a function of pH_o is explained as the sum of the transport by two routes, (a) and (b) (see Fig. 1); the chloride transport by each route is demonstrated in Fig. 15 with (*A*) low (30 mM) and (*B*) high (330 mM) [Cl]. The transport by route (a) is the normal exchange at neutral pH_o. The transport by this path gradually declines by deprotonation of a group with an intrinsic pK of ~9.4. Since this deprotonation is substrate sensitive, the apparent pK for this inactivation of system (a) changes from ~9.6 to ~10.7, with increasing $[Cl_o]$ from 2 to 165 mM and $[Cl_i] = 165$ mM. Concomitant with the decline of system (a) the alkaline transport

function (b) is activated. This activation changes the asymmetry factor from ~10 to ~0.2, indicating recruitment of unloaded sites from the intracellular to the exofacial side of the membrane and an increase in the chloride binding constant K_{Cl} from ~30 to ~110 mM. Moreover, the maximal translocation rate increases by a factor of almost 1.7. The activation of route (b) is changed into inactivation as the deprotona-

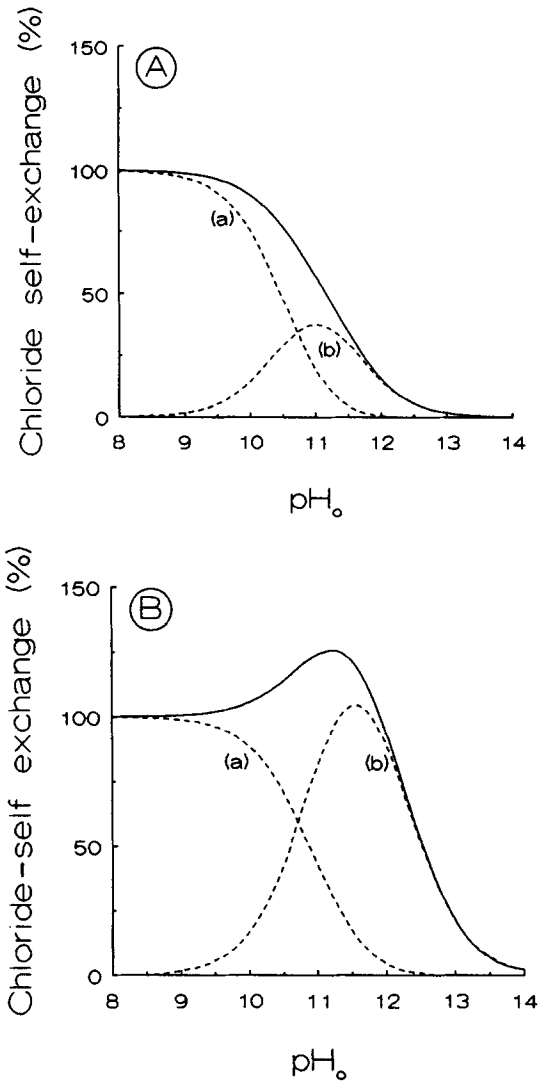

FIGURE 15. Interpretation of the transport model. Chloride self-exchange is the sum of the two transport functions, namely, the system at neutral pH (a) and at alkaline pH (b). *A* shows the theoretical normalized curves obtained from the constants in Table III, with $[Cl_o] = [Cl_i] = 30$ mM, and *B* with $[Cl_o] = [Cl_i] = 330$ mM. The modifier hump is thus explained by a higher maximal translocation rate (J^b_{max}) in the alkaline system.

tion of the second group with an intrinsic pK of 11.35 becomes dominant. Deprotonation of this second group, which is also chloride sensitive, apparently completely abolished anion exchange (cf. Figs. 2 *C*, 9, and 10). The importance of this group in anion binding can be derived from the result of Fig. 6 *B*, the apparent pK_{alk} determined as a function of $[Cl_o]$ (Fig. 10), and from the K_o^{app} as a function of pH_o

(Fig. 13 *A*). The transportation by the alkaline system (b) as a function of pH_o demonstrates a bell-shaped configuration with a $[Cl_o]$-dependent optimum. At higher $[Cl_o]$ (> 100 mM) this optimum becomes significant in the total transport function (see Fig. 15) and is responsible for the appearance of the modifier hump first described by Wieth and Bjerrum (1982). The pH_o at the alkaline optimum of system (b) is not constant but elevates slightly, for example, from pH ~10.9 to pH ~11.4 when $[Cl_o]$ is raised 2–165 mM with $[Cl_i]$ = 165 mM. Besides fitting the data in Figs. 9–13, the model also fits the data obtained at high ionic strength by Wieth and Bjerrum (1982) as demonstrated in Figs. 2 *B*, 9, 10, and 14 *B*).

In the development of the transport equation it was assumed that binding of the transported anion is a fast process compared with the translocation step. This assumption is supported by NMR studies (Falke and Chan, 1985). The proposed model scheme (Fig. 1) is based on two more essential assumptions. The first is that the exofacial groups are only sensitive to changes in the alkaline pH_o when the transport site faces outward. The second is that no change in protonation of these groups apparently takes place from the intracellular side when the transporter is recruited inward. The first statement is indirectly proven by the fit of the model to the experimental data with various chloride gradients across the membrane (cf. Figs. 11 and 12). Deviations from the model are nevertheless obtained with stronger inward recruitment of the transporter (data not shown), indicating that extracellular titration of the inward-facing forms may become significant under such conditions. The second statement is justified by the observation of Wieth and Bjerrum (1982) that the proton efflux at pH_o 12.4, pH_i 7.2, and $[Cl_o] = [Cl_i]$ = 165 mM at 0°C was only 3% of the measured chloride self-exchange efflux of 150 pmol cm^{-2} s^{-1}. A nearly 100% efflux-cotransport of intracellular protons is to be expected if intracellular reprotonation of the pK_4 groups takes place. Moreover, when the pK_5 is concerned, this group does not appear to be reprotonated from the intracellular site for the same reason. The empty S_o may, of course, slowly reorient to an empty inward-facing form resulting in an overall coupled efflux of chloride and protons. For this mechanism to be of importance for model interpretation, the "leak" should be substantial and such leaks are not observed at alkaline pH_o (see Figs. 9–12). Another possibility is that the S_o form may transport anions but only binds chloride with a very low affinity (see Fig. 2 *B*). In this case the S_oCl_o form may or may not reprotonate when changed into the inward-facing form, but if it does it will only transport protons to an insignificant degree due to a negligible $[S_oCl_o]$. None of these possibilities is thus for a quantitative reason in conflict with the model assumption, that the pK_5 group can only be titrated from the exofacial side.

The observed disagreements between the theoretical alkaline pK values pK_{ts} and pK_{alk}, as a function of $[Cl_o]$ in the paper by Wieth and Bjerrum (1982) and in this presentation, are due to the different model interpretations which influence the way the alkaline pK's are calculated. In the paper by Wieth and Bjerrum (1982; their Fig. 10), the apparent pK_{ts} value reached a constant value at $[Cl_o]$ > 165 mM. The same is observed for the data presented here if the definition for pK_{ts} is used. The apparent pK_{ts} values at 165, 330, 500, and 660 mM [Cl] are thus 11.9, 12.0, 12.1, and 12.0, respectively. These pK values are very different from the apparent theoretical alkaline pK values (pK_{alk}) defined in relation to the new model. The

discrepancy is obtained because it is assumed in the old model that the modifier effect gradually disappears at alkaline pH_o, whereas it stays constant in the new model due to the intracellular location of the Dalmark modifier site. These pK_{alk} values are defined as the pH_o at which the transport is half of the theoretical maximal alkaline transport value at a given $[Cl_o]$ and $[Cl_i]$. The maximal value represents the calculated chloride self-exchange in a theoretical situation where the group with a pK of 9.4 is not protonated at low pH. The model values can be derived from Eq. T10 as:

$$pK_{alk} = \log(\{1 + [Cl_0]\cdot((A^b + 1)/K_{Cl}^b)\cdot(1 + ([Cl_i]/K_m)) + (A^b/[Cl_i])\}/K_5) \qquad (R1)$$

When this definition is used and a value for J_{max}^b of 726 pmol cm^{-2} s^{-1} is assumed, the apparent pK_{alk} from the experimental data at 165, 330, 500, and 660 mM $[Cl_o]$ becomes 12.0, 12.25, 12.5, and 12.65, respectively. These values, which increase steadily with log ($[Cl_o]$), are close to the theoretical values calculated from Eq. R1 as demonstrated by the fit to the model (dashed curves, Fig. 10) obtained from the compiled constants in Table III. The result indicates that pK_{alk} increases nearly linearly with log ($[Cl_o]$) over the range examined.

Ionic Strength Effects

The first deprotonatable group (with pK_4) has an intrinsic (when no chloride is bound) pK of ~9.4 (cf. Fig. 5) at constant high ionic strength. The apparent pK value was lowered ~0.5 pK units at ~1.8 mM KCl (Fig. 2 *C*) and 0.35 pK units at 5 mM KCl (Fig. 2 *A*) without citrate present. The alteration in pK could not be explained by a direct citrate inhibitory effect because this would not explain the intersection of the two titration curves in Fig. 2 *A*, indicating stimulation of chloride self-exchange in the presence of citrate. The change in pK of ~0.35 pK units at 5 mM Cl_o should be compared with a value of ~0.05 pK units found by model calculation with citrate binding to the S_oH_2 form with an intrinsic competitive inhibitor constant of ~60 mM (Liu and Knauf, personal communication) and a 10-fold lower affinity for the S_oH form. Even assuming the same affinity for citrate to both forms (K_{inh} ~60 mM) will only change the pK ~0.15 units. The influence of citrate on the apparent pK is therefore considered to be mainly an electrostatic event deriving from the free citrate ions in the solution, and to a much lesser extent a competitive effect. This statement represents a revision of the Wieth and Bjerrum (1982) conclusion that citrate is completely excluded from the transport domain at $pH_o > 8$. The former conclusion was based on experiments with $[Cl_o] > 16$ mM, where ionic strength effects are less pronounced and competitive inhibition is negligible. The fact that the value of K_o^{app} (RBC) at pH 7.0 (0.45 mM) at low ionic strength (see legend to Fig. 2 *C*) is much lower than the value of K_o^{app} (also obtained with RBC) at pH 8 in the presence of citrate (1.2 mM) cannot be explained simply by competitive inhibition by trivalent citrate, since the increase in K_o^{app} with citrate present should be only ~40% using the intrinsic inhibition constant for citrate of ~60 mM, pH_o 8, 0°C (Liu and Knauf, personal communication). It therefore appears that the chloride binding constant is also altered (by a factor of ~2) by the change in the ionic strength.

Ionic strength effects on the K_{Cl} value are also observed. A K_{Cl} value of ~50 mM, obtained by Gasbjerg and Brahm (1991), without compensation for change in the

ionic strength, should be compared with the K_{Cl} value of ~30 mM reported here. The Gasbjerg and Brahm (1991) value was obtained by assuming modifier effects not only on the loaded but also on the unloaded forms, but this difference has nearly no influence on the K_{Cl} determination. This discrepancy between the K_{Cl} value is in the opposite direction of what should be expected from citrate inhibition and/or ionic strength effect on simple electrostatic binding. The disagreement between the two K_{Cl} values can nevertheless be rationalized as an ionic strength effect if it is assumed that the rate constants for inward and outward translocation of the loaded forms are more sensitive to changes in ionic strength than the intrinsic chloride dissociation constants.

Since it was found that ionic strength has a strong effect on the different constants, the ionic strength was kept constant whenever possible in the experiments reported here. The citrate used introduces an error in the determined constants, due to a direct citrate competition at the binding site. This effect is substantial with respect to monovalent and divalent citrate anions, which are dominating at pH <7–8, but appear to be of minor importance at alkaline pH (pH >8) (see Results, Fig. 2) where the trivalent form (with much low affinity for the binding site) is dominant (Liu and Knauf, personal communication). An explanation for this low citrate affinity at pH >8 could be that trivalent citrate is repelled to some extent from the binding site region due to a surplus of negative charge, if this region (as discussed below) consists of maximally two positive groups located in a hydrophobic environment.

The pK_4 value at low ionic strength was estimated (from Fig. 2 *C*) to be 8.7–8.8 using the method described in relation to Fig. 5. This value is close to the value of the deprotonatable group which has been identified by competitive iodide inhibition of chloride self-exchange at alkaline pH_o and low ionic strength (Liu and Knauf, 1990) and apparently corresponds to the same group. The very strong ionic strength effect on the pK_4 group (0.7 pK unit when changing the ionic strength from 150 toward 0 mM) is consistent with a hydrophobic location of this group (as proposed below), because ionic strength effects are strongly increased in a medium with low dielectric constant.

Modifier Effects

The intracellular modifier effect first described by Dalmark (1976) is also included in the model equation. This modifier effect was earlier assumed to be a simple noncompetitive effect (Gasbjerg and Brahm, 1991). The ping-pong parameters obtained from the presented data at neutral pH with a simple noncompetitive modifier effect (involving all terms) gave slightly different values of K^a_{Cl} (31.7 mM), K_m (426 mM), and J_{max} (478 pmol cm^{-2} s^{-1}), but a more significant change in A, which increased to 15.3. When these values were used in model calculations they gave a significantly poorer fit to the experimental data than the values compiled in Table III. It thus appear that the intracellular modifier effect is most significant on the inward-facing (chloride-loaded) transport form. For the sake of simplicity it was assumed in the Theory section that chloride self-inhibition only acts on the loaded forms. This assumption is not formally different from the assumption of self-inhibition of the loaded inward-facing form only.

Functional and Structural Aspects of the Model

The establishment of the kinetic model does not prove that the essential part of the exofacial anion binding site is actually composed of two positive groups, but only that this appears to be the simplest model that can explain the experimental results. Several more groups acting in concert may give a similar titration pattern. Yet assuming that only two groups are involved, one or both of the groups may only influence the binding allosterically, because it is not necessary to assume that the deprotonatable groups influence each other electrostatically or even allosterically to obtain the observed kinetics. These conclusions can be stated from Fig. 16 (see below), from the intersection between the curve $K_i/K'_i = 1$ and the abscissa. This intersection (indicated by the arrow) represents conditions where the change from the (a) to the (b) state is obtained by an alteration in K_{ex} from 105 to 1.96 without changes in the intrinsic chloride constants $K_o = K'_o = 271$ mM, $K_i = K'_i = 27.7$ mM, and $pK_4 = pK_3 = 9.36$. However, the condition, although possible, appears unlikely because $K_o \gg K_i$, in contrast to the intrinsic dissociation constants for iodide or sulfate (determined as competitive inhibitor constants) which are found to behave opposite (Schnell, Gerhardt, and Schoppe-Fredenburg, 1977; Knauf, Mann, Brahm, and Bjerrum, 1986).

Despite the fact that it is not possible for theoretical reasons (Stein, 1981) to determine most of the intrinsic constants K_o, K'_o, K_3, K_i, K'_i, K^a_{ex}, and K^b_{ex} of this model from steady-state experiments, it is, on the other hand, possible to estimate some limits for these constants from the reported experiment with iodide as a competitive extracellular inhibitor. From the values obtained for K^I_o, $K^{I'}_o$, and K_4 it is possible to calculate the value of pK_6 by the relation $K_4 \cdot K^I_o = K_6 \cdot K^{I'}_o$ (see Fig. 1) to be ~ 11. This value indicates that the pK of the first deprotonatable group (with a pK of ~ 9.4) is increased by ~ 1.5 pK units when an iodide ion is bound at the transport site. Since the binding site is assumed to interact through charge interactions with the transported ions, the expected effect of chloride should not be much different from the effect of iodide, indicating that $pK_3 - pK_4$ should be ~ 1.5 pK unit. According to the ping-pong kinetics (Knauf et al., 1984; Fröhlich and Gunn, 1986), we have:

$$K_o = K_{Cl} \cdot (K_{ex} + 1)/(A + 1) \tag{D1a}$$

and

$$K_i = K_o \cdot A/K_{ex} \tag{D1b}$$

From these equations, which can be applied to both the (a) and (b) systems, the difference in pK between pK_3 and $pK_4 = \log (K'_o/K_o)$ can be expressed as a function of $\log (K^a_{ex})$ at different values of the ratio K'_i/K_i, using the value for K^a_{Cl}, K^b_{Cl}, A^a, and A^b obtained in Table III. The correlation at different values of the ratio K'_i/K_i equal to 0.5, 0.66, 1, 1.5, and 10 is shown in Fig. 16. If it is assumed that the system is unlikely to function in a metastable situation where a small change in K'_i/K_i gives a large change in the other parameters (as for $K'_i/K_i < 1$) and if it is assumed that the change in pK, when binding a chloride ion, is comparable to that observed from binding iodide (probably not less than 1.3 pK units), it can be concluded that $K_i \leq K'_i$ and $K^a_{ex} < 2.5$ (Fig. 16, dashed vertical line). From these limitations it can be

calculated that 2.5 mM $< K_o <$ 9 mM and $K_i >$ 38 mM. The values for the (b) system under the same conditions can be estimated to be $K^b_{ex} < 0.9$, 90 mM $< K'_o <$ 180 mM, and $K'_i >$ 38 mM. This estimated limitation for the involved intrinsic constants indicates that the pK's of both groups are changed when an anion is bound. Moreover, both groups appear to interact electrostatically and to be involved in anion binding because $K_o \ll K'_o$.

Concerning the chemical nature of the two groups, the group with the higher pK (11.35) is likely to be an arginine residue (Wieth et al., 1982*b*; Bjerrum et al., 1983). It has a low pK value for an arginine but could be influenced by a hydrophobic environment (the substrate binding site is proposed to be located within the membrane (Rao, Reithmeier, and Cantley, 1979; Schnell, Elbe, Kasbauer, and Kaufmann, 1983). The first deprotonatable group (pK ~9.4) is more likely to be a lysine group, as estimated from the pK value. This group could represent the

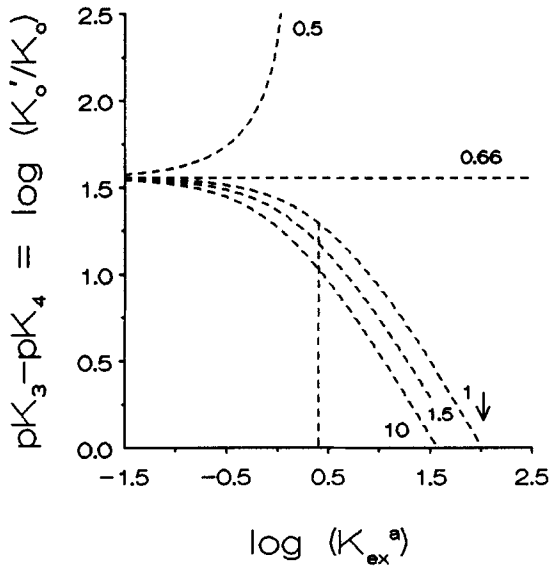

FIGURE 16. The theoretical relation between pK_3–pK_4 = log (K'_o/K_o) and log (K^a_{ex}). The dashed lines show the theoretical relations assuming different values (0.5–10) for the ratio K'_i/K_i. When this ratio is <1, the system appears to be in a metastable situation. The arrow indicates a situation where $K_o = K'_o$, $K_i = K'_i$, and $pK_3 = pK_4$ (see text for details).

functionally important lysine group, which also reacts irreversibly with H_2DIDS (Jennings, Mornaghan, Douglas, and Nicknish, 1985). An arginine, however, cannot be ruled out due to a very selective phenylglyoxal (PG) labeling of one binding site group at low [Cl_o] (Bjerrum et al., 1983; Bjerrum, 1989*a*), indicating that at least one of the two possible functionally PG reacting arginine groups may have a very low pK value (Patty and Thész, 1980). The pK_4 group could be this arginine group with an unusual low pK if the group is located in a hydrophobic environment and interacts closely with the second deprotonatable group as explained below.

If two positively charged protonated groups are placed close together, their willingness to undergo deprotonation will be increased. This is mainly due to the charge repulsion which depends on the mean dielectric constant (ϵ) and the distance between the charges (Schwarzenbach, 1970). Making certain simplifying assumptions (only taking electrostatic interactions into account), the relation between ϵ, distance,

and ΔpK can be estimated theoretically as first described by Bjerrum (1923). Assuming a moderate reduction in ϵ to 30 at the binding site (see below) and a distance between the charges of 5 Å, a mutual reduction in pK of ~2 pK units will be obtained. Charged groups located in a hydrophobic cavity will, moreover, be decreased in pK solely by the hydrophobic localization. The decrease in pK when ϵ is reduced from 80 to 30–35 can be estimated to be ~2 pK units. Based on these considerations, it is not inconceivable that an arginine with a pK of ~13 in free solution may be reduced by as much as ~4 pK units (to pK ~9) when located in a hydrophobic cleft with these conditions and low $[Cl_o]$.

Besides being responsible for a well-defined arrangement of the charged groups in the binding site region (Carlton, 1982), the hydrophobic region would also increase the affinity for anion binding. An estimate of the intrinsic binding constant K_o for monovalent anions to the transport site based on the above-mentioned presumptions, as well as on the assumption that only electrostatic interactions are important (assuming that the charges of the binding site can be regarded as a simple point charge), can be derived from the equation:

$$1/K_o = \int_a^d 4{,}000\pi N_a r^2 \exp\left[|-z_1 z_2| e^2/(4\pi\epsilon\epsilon_0 rkT)\right] dr \qquad \text{(D2)}$$

TABLE IV

Z_1–Z_2	ϵ = 30		ϵ = 35		ϵ = 80	
	(2-1) K_o	(1-1) K'_o	(2-1) K_o	(1-1) K'_o	(2-1) K_o	(1-1) K'_o
			mM			
4 Å	0.38	19.6	1.16	39.2	72.0	∞
5 Å	0.92	27.4	2.18	56.0	108.3	∞
6 Å	1.46	37.0	3.12	81.2	181.3	∞

developed by Bjerrum (1926), where z_1 and z_2 are the charge numbers of the interacting charges of the binding site and the anion, respectively, r is the variable distance between the center of the two charges and the anion, e is the elementary charge, ϵ_o is the dielectric constant in vacuo, N_a is Avogadro's number, T is the absolute temperature, k is the Boltzmann constant, a is the shortest distance between the group(s) and the anion, $d = |z_1 z_2|\ e^2/(8\pi\epsilon\epsilon_0 kT)$ is the distance for which the equation inside the integration sign in Eq. D2 gives a minimum (see Bjerrum, 1926). The theoretical K_o and K'_o (calculated by numerical integration) at 0°C, ionic strength = 0, at an ϵ value of 30, 35, and 80, as a function of the shortest distance a (in ångströms) between the ion and the binding site groups were as shown in Table IV.

These different calculated K_o values (with ϵ equal to 30–35) are of the right order of magnitude for the iodide binding constants K_o^I and $K_o^{I'}$ determined here and probably also for the corresponding chloride constants, assuming a distance between the groups of 4–5 Å. For a direct quantitative comparison, the ionic strength effect, solvation energy, and local configuration of the binding site should also be taken into account. The hypothesis that electrostatic interactions are the main force in binding of anions indicates that the experimentally observed affinity for iodide, for example,

is only likely if ϵ is reduced at the binding site (independent of whether the binding groups are lysine, arginine, or two arginines) as judged from the calculated binding affinities. The K_o values at $\epsilon = 80$ demonstrate that such a high value for ϵ is only likely with stronger electrostatic interactions (for example, three or more interacting groups).

From the model fits to the experimental data with an inwardly directed gradient (Figs. 11 and 12) it can be concluded that the deprotonatable exofacial groups are not very accessible for deprotonation from the extracellular side when the transport sites are located inward. Moreover, it was concluded that at least the K_4 group (but probably both groups) are not titrated from the intracellular side. An explanation could be that the pK_o increases substantially (1–2 pK units) for both groups with inward translocation of the transport system. An increase in pK_o could result from a local increase in ϵ around the group(s) or an alteration in the electric potential in the environment of the group(s) from an approaching carboxyl group. Such a group could increase the pK, "push" the translocating chloride ion from the exofacial binding site during the inward translocation, and remove exofacial substrate affinity. A likely candidate for the carboxyl group could be the functionally important group recently identified by Jennings and Al-Rhaiyel (1989) with Woodward's reagent, but the carboxyl identified by Bjerrum, Andersen, Borders, and Wieth (1989) with the carbodiimide EAC may also be a possibility. Yet another mechanism is translocation of at least one of the protonatable groups (probably the pK_5 group) with the transported anion as proposed by Bjerrum (1989*a*, *b*). In this case the other positive group would be left on the exofacial side with a significantly increased pK value. A combination of the carboxyl and the pK_5 group translocation mechanisms is also a possibility.

Effects of Inhibitors on Alkaline Titration

The observed transport stimulation at alkaline pH, the modifier hump, is interpreted as being due to titration of a group which changes the translocation rate of the transport system (see Fig. 15). The same mechanism together with a reduction in inhibitor affinity with alkaline pH_o can also explain the more pronounced appearance of a hump in the presence of extracellular inhibitors such as iodide (see Fig. 14 *B*). A similar but broader hump is seen with most other inhibitors as well, including DNDS, salicylate, and niflumic acid (data not shown). The stimulation of chloride self-exchange at alkaline pH_o, in the presence of the more bulky inhibitors that compete with chloride, begins at lower pH and apparently involves titration of additional positive groups with pK values between 8 and 10. Deprotonation of these accessory binding groups, which are likely to be lysine groups, has only a small effect on chloride transport itself, but strongly reduces the affinity of the inhibitor. Iodide inhibition at alkaline pH_o can be explained simply by assuming that I_o competes reversibly with chloride for the S_oH and S_oH_2 forms. The fit to the iodide data (Fig. 14 *B*) was obtained using the extracellular modifier constant K_m^I obtained in Fig. 14 *A*. The obtained values for $K_o^I \approx 1$ mM and $K_o^{I'} \approx 38$ mM are remarkably similar to the respective dissociation constant values for iodide binding at alkaline pH obtained by another method (Liu and Knauf, personal communication).

In conclusion, the effect of extracellular deprotonation of the transport system on chloride self-exchange can be described by a "simple" kinetic model involving two deprotonatable binding groups. Deprotonation of one of these groups changes the transport system from the neutral to the alkaline state, which still shows ping-pong kinetics but which has different parameters. Titration of the second group appears to arrest translocation completely. Whether the groups proposed in the model correspond to two existing groups which bind the transported anion or are traceable to more complicated allosteric interactions between several groups cannot be established definitively by kinetic experiments, and more evidence concerning the structure of the anion transport pathway is required before this question can be resolved.

Lise Mikkelsen, Anne Dorthe Davel, Aase Valsted, and Ulla Lange are thanked for valued technical assistance. Dr. P. Gasbjerg is thanked for comments and Dr. P. A. Knauf for critical reading and constructive criticism of the manuscript.

Original version received 4 June 1991 and accepted version received 20 April 1992.

REFERENCES

Bjerrum, N. J. 1923. Dissoziationskonstanten von mehrbasischen Säuren und ihre Anwendung zur berechnung molekularer Dimensionen. *Zeitschrift für Physicalische Chemie.* 106:219–242.

Bjerrum, N. J. 1926. Untersuchungen über Ionenassoziation. I. Der Einfluss der Ionenassoziation auf die Aktivität der Ionen bei mittleren Assoziationsgraden. *Det Kongelige Danske Videnskabernes Selskab. Mathematisk-fysiske Meddelelser VII.* 9:1–48.

Bjerrum, P. J. 1989*a*. Chemical modification of the anion transport system with phenylglyoxal. *Methods in Enzymology.* 173:466–494.

Bjerrum, P. J. 1989*b*. Irreversible modification of the anion transporter. *In* The Red Cell Membrane. B. U. Raess and G. Tunicliff, editors. The Humana Press, Inc., Clifton, NJ. 329–367.

Bjerrum, P. J., O. S. Andersen, C. L. Borders, Jr., and J. O. Wieth. 1989. Functional carboxyl groups in the red cell anion transport protein. *Journal of General Physiology.* 93:813–839.

Bjerrum, P. J., J. O. Wieth, and C. L. Borders, Jr. 1983. Selective phenylglyoxalation of functionally essential arginyl residues in the erythrocyte anion transport protein. *Journal of General Physiology.* 81:453–484.

Cabantchik, Z. I., and A. Rothstein. 1974. Membrane protein related to anion permeability of human red blood cells. I. Localization of disulfonic stilbene binding sites in protein involved in permeation. *Journal of Membrane Biology.* 15:207–226.

Carlton, H. P. 1982. Building models of globular protein molecules from their amino acid sequences. *Journal of Molecular Biology.* 155:53–62.

Dalmark, M. 1976. Effect of halides and bicarbonate on chloride transport in human red blood cells. *Journal of General Physiology.* 67:223–234.

Dalmark, M., and J. O. Wieth. 1972. Temperature dependence of chloride, bromide, iodide, thiocyanate and salicylate transport in human red cells. *Journal of Physiology.* 244:583–610.

Falke, J. F., and S. I. Chan. 1985. Evidence that anion transport by band 3 proceeds via a ping-pong mechanism involving a single transport site. A ^{35}Cl NMR study. *Journal of Biological Chemistry.* 260:9537–9544.

Fröhlich, O., and R. B. Gunn. 1986. Erythrocyte anion transport: the kinetics of a single obligatory exchange system. *Biochimica et Biophysica Acta.* 864:169–194.

Funder, J., and J. O. Wieth. 1976. Chloride transport in human erythrocytes and ghosts: a Quantitative comparison. *Journal of Physiology.* 262:679–698.

Gasbjerg, P. K., and J. Brahm. 1991. Kinetic of bicarbonate and chloride transport in human red cell membranes. *Journal of General Physiology.* 97:321–349.

Gunn, R. B., and O. Fröhlich. 1979. Assymetry in the mechanism of anion exchange in human red blood cell membranes. Evidence for reciprocating sites that react with one transported anion at a time. *Journal of General Physiology.* 74:351–374.

Jennings, M. L., and S. Al-Rhaiyel. 1989. Modification of carboxyl group that appears to cross the permeability barrier in the red blood cell anion transporter. *Journal of General Physiology.* 92:161–178.

Jennings, M. L., R. Mornaghan, S. M. Douglas, and J. S. Nicknish. 1985. Function of extracellular lysine residues in the human erythrocyte anion transport protein. *Journal of General Physiology.* 86:653–669.

Knauf, P. A., F.-Y. Law, T. Tarshis, and W. Furuya. 1984. Effects of the transport site conformation on binding of external NAP-taurin to the human erythrocyte anion exchange system. *Journal of General Physiology.* 83:683–701.

Knauf, P. A., and N. A. Mann. 1984. Use of niflumic acid to determine the nature of the asymmetry of the human erythrocyte anion exchange system. *Journal of General Physiology.* 83:703–725.

Knauf, P. A., and N. A. Mann. 1986. Location of the chloride self-inhibitory site of the human erythrocyte anion exchange system. *American Journal of Physiology.* 251 (*Cell Physiology* 20):C1–C9.

Knauf, P. A., N. Mann, J. Brahm, and P. J. Bjerrum. 1986. Asymmetry in iodide affinities of external and internal facing red cell anion transport sites. *Federation Proceedings.* 45:1005.

Knauf, P. A., N. A. Mann, J. E. Kalwas, L. J. Spinelli, and M. Ramjeesingh. 1987. Interaction of NIP-taurine, NAP-taurine, and Cl− with the human erythrocyte anion exchange system. *American Journal of Physiology.* 253:C652–C661.

Liu, S.-Q., and P. A. Knauf. 1990. Evidence from pH effects that amino acids other than arginine affect substrate affinity of the external-facing transport site of human erythrocyte band 3. *Biophysical Journal.* 57:89*a*. (Abstr.)

Milanick, M. A., and R. B. Gunn. 1986. Proton inhibition of chloride exchange Asynchrony of band 3 proton and anion transport sites? *American Journal of Physiology.* 250:C955–C969.

Patty, L., and J. Thész. 1980. Origin of selectivity of α-dicarbonyl reagents for arginyl residues of anion binding sites. *European Journal of Biochemistry.* 105:387–393.

Rao, A. R., R. A. F. Reithmeier, and C. L. Cantley. 1979. Location of distilbene disulfonate binding site of the human erythrocyte anion exchange system by resonance energy transfer. *Biochemistry.* 18:4505–4516.

Schnell, K. F., W. Elbe, J. Kasbauer, and E. Kaufmann. 1983. Electron spin resonance studies on the inorganic-anion-transport system of the human red blood cell: binding of a disulfonate stilbene spinlabel (NDS-Tempo) and inhibition of anion transport. *Biochimica et Biophysica Acta.* 732:266–275.

Schnell, K. F., S. Gerhardt, and A. Schoppe-Fredenburg. 1977. Kinetic characteristics of the sulfate self-exchange in human red blood cells and red blood ghosts. *Journal of Membrane Biology.* 30:319–350.

Schwarzenbach, G. 1970. Electrostatic and non-electrostatic contributions to ion association in solution. *Pure and Applied Chemistry.* 24:307–334.

Stein, W. D. 1981. Concepts on mediated transport. *In* Membrane Transport. F. M. A. H. Schurrmans Stekhoven and S. L. Bonting, editors. Elsevier, North-Holland Biomedical Press, Amsterdam. 123–158.

Weast, R. C. 1987. Handbook of Chemistry and Physics. CRC Press, Inc., Boca Raton, FL. D219–D269.

Wieth, J. O., O. S. Andersen, J. Brahm, P. J. Bjerrum, and C. L. Borders, Jr. 1982*a*. Chloride-bicarbonate exchange in red blood cells and chemical modification of binding sites. *Philosophical Transactions of the Royal Society of London B Biological Sciences.* 299:383–399.

Wieth, J. O., and P. J. Bjerrum. 1982. Titration of transport and modifier sites in the red cell anion transport system. *Journal of General Physiology.* 79:253–282.

Wieth, J. O., and P. J. Bjerrum. 1983. Transport and modifier sites in capnophorin, the anion transport protein of the erythrocyte membrane. *In* Structure and Function of Membrane Proteins. E. Quagliaiello and F. Palmieri, editors. Elsevier Science Publishers, Amsterdam. 95–106.

Wieth, J. O., P. J. Bjerrum, and C. L. Borders, Jr. 1982*b*. Irreversible inactivation of red cell chloride exchange with phenylglyoxal. An arginine specific reagent. *Journal of General Physiology.* 79:283–312.